Geologica Acta, Vol.3, Nº2, 2005, 81-106
Available online at www.geologica-acta.com

geologica acta

Late Triassic to Early Jurassic sedimentation in northern Neuquén Basin, Argentina: Tectosedimentary Evolution of the First Transgression

S. LANÉS

CONICET-Departamento de Geología, Universidad de Buenos Aires
Intendente Güiraldes 2620, Ciudad Universitaria, Pabellón 2, 1º piso, 1428 Buenos Aires, Argentina.
E-mail: lucero_sil@yahoo.com.ar

ABSTRACT

The present paper interprets and discusses the Late Triassic-Early Jurassic of the first transgression at northern Neuquén basin (Argentina) and its paleostructural control due to ancient horsts and half-grabens. Six vertical sections were chosen along two east-west and north-south transects. Depositional systems have been determined and correlated by means of ammonite, bivalve and brachiopod biostratigraphy. Two regions can be distinguished based on the areal distribution of the contemporaneous depositional systems in the studied area; one at the east and the other to the west of El Freno creek. Vertical sections in the western region record shallowing-upward fluvio-dominated, transverse, normal-fault-controlled, slope-type fan deltas and intermediate shelf to Gilbert-type fan deltas. Vertical sections in the eastern region record a transgressive siliciclastic storm-dominated shelf, evolving from wave-dominated estuary to turbidity current influenced outer shelf. Accommodation vs. sedimentary supply ratio leads to identification of two stages of differing tectonic behaviour. The first one (Rhaetian-late Early Sinemurian) shows an accomodation greater than the sedimentary supply leading to the deposition of the western slope-type fan deltas. The second stage (late Early Sinemurian-Toarcian) shows a varying accommodation: during the late Early Sinemurian, accommodation was outpaced by sedimentary supply leading the intermediate-type fan delta to prograde. Later (late Early Sinemurian-Toarcian), accommodation exceeded the supply again, allowing transgression of the marine shelf and the increase in the marine depositional area. The two stages coincided with synrift and sag phases previously proposed for the southern Neuquén basin.

KEYWORDS | **Upper Triassic. Lower Jurassic. Sedimentology. Tectonics. Neuquén Basin.**

INTRODUCTION

The Neuquén Basin is a Mesozoic oil-bearing basin filled with more than 6000 m of marine and continental sedimentary rocks (epiclastics, carbonates, evaporites and volcaniclastics) of Late Triassic to Eocene age (Gulisano and Gutiérrez Pleimling, 1994; Legarreta and Gulisano, 1989).

This basin originated from a series of unconnected asymmetric north-south trending half-grabens (Vergani et al., 1995; Manceda and Figueroa, 1993, 1995; Tankard et

© UB-ICTJA

al., 1995) during rifting in the Middle Triassic-Sinemurian (Ramos, 1992; Manceda and Figueroa, 1995), when the non-marine, mainly non-fossiliferous, siliciclastic and volcanic deposits (Gulisano, 1981; Gulisano et al., 1984; Legarreta and Gulisano, 1989) filled the unconnected half-grabens in the basin margins. At the same time, the basin center was rapidly transgressed by nearshore sandstones and offshore shales (Gulisano, 1981) partly due to the Sinemurian to Toarcian (Vergani et al., 1995) regional sag phase which caused the unconnected half-grabens to coalesce in the Pliensbachian (Legarreta and Gulisano, 1989) when most of the basin was transgressed. The unconnected half-grabens locally controlled the beginning of the transgression and the partial synchronism between continental and marine units of Late Triassic-Early Jurassic age (Gulisano, 1981; Gulisano and Gutiérrez Pleimling, 1994).

The purpose of the present paper is to interpret and discuss the tectosedimentary evolution of the Atuel valley sections during the Late Triassic-Early Jurassic and its likely structural controls in order to enhance the future correlations of the non-marine and marine units above. One of the impediments to reliable correlations is the lack of fossils of biostratigraphic value in the underlying non-marine units because they are usually dated through field stratigraphic relationships and the biostratigraphic content of the overlying transgressive deposits.

The Atuel valley region is a palentological and stratigraphic classic locality of the Lower Jurassic of the Neuquén basin (Bodenbender, 1892; Wehrli and Burckhardt, 1898; Behrendsen, 1921; Steuer, 1921; Jaworski, 1925; Gerth, 1925; Groeber, 1946, 1947; Reijenstein, 1967; Stipanicic, 1969; Stipanicic and Bonetti, 1970; Volkheimer, 1978; Damborenea, 1987, 2002; Riccardi et al., 1988, 1991, 1997; Riccardi and Iglesia Llanos, 1999). All the litostratigrahic units valid for the northern Neuquén basin were defined here (Stipanicic, 1969; Stipanicic and Bonetti, 1970; Volkheimer, 1978; Riccardi et al., 1997). However, the detailed sedimentological, paleoenvironmental and tectonic features of the area remains unknown.

The adequacy of the Atuel valley region for the present study is based on three facts. First, it hosts the oldest Late Triassic (Riccardi et al., 1997) record of the first transgression which began in the Early Pliensbachian in most of the basin. Second, the transgressive marine deposits here contain a varied fauna of ammonites, bivalves and brachiopods, which allow datation and biostratigraphic correlations. And finally, the transgressive deposits show strong lateral changes of facies and age with muddier and older (Late Triassic-late Early Sinemurian) transgressive accumulations in the west part of the study area and the sandier and younger (late Early Sinemurian-Toarcian) ones in the eastern part. Determination of the origin and controls of such changes was the core of the present study and the base to the local paleogeographic model and tectosedimentary evolution presented here.

GEOLOGICAL SETTING

The Neuquén Basin is a Mesozoic back-arc basin on the western convergent margin of the South American plate (Legarreta and Gulisano, 1989) and is attributed to the extension during the fragmentation of Gondwana and the opening of the South Atlantic Ocean (Uliana and Biddle, 1988). The earliest episode of rifting, during the Middle Triassic-Sinemurian (Ramos, 1992; Manceda and Figueroa, 1995), formed a series of unconnected north-south trending asymmetric half-grabens bound by basement-involved faults (Vergani et al., 1995; Manceda and Figueroa, 1993, 1995; Tankard et al., 1995) which controlled the subsidence and sedimentation. A consequent regional sag phase during the Sinemurian to Toarcian (Vergani et al., 1995) led the unconnected half-grabens to coalesce in the Pliensbachian (Legarreta and Gulisano, 1989) and most of the Neuquén basin was transgressed. Features, areal distribution and basal age of the sag deposits depended on a marked basement topography, which was apparently controlled by the main faults and horsts, though the detailed structural pattern remains unknown (Manceda and Figueroa, 1995). The unconnected half-grabens also locally controlled the beginning of the transgression and the partial synchronism between continental and marine units of Late Triassic-Early Jurassic age (Gulisano, 1981; Gulisano and Gutiérrez Pleimling, 1994) because the continental deposits filled the marginal depocenters while the center of the basin was rapidly transgressed (Gulisano, 1981). Transgressive deposits include nearshore sandstones and offshore shales of Early Pliensbachian-Middle Callovian age in most of the basin. In southern Mendoza, in the northern Neuquén basin, a remarkable feature of these transgressive deposits is the retrogradational pattern and a strong increase of their depositional area due to the combination of regional thermal subsidence together with the global eustatic sea level rise in the Early Jurassic (Legarreta et al., 1993).

The study area (between 34° 39´ and 34° 56´S and 69° 41´and 69° 54´W) extends from the easterly Blanco creek at the north, to the northern margin of the Atuel river (between Malo and Blanco creeks) at the south (Fig. 1). It belongs to the Atuel-Valenciana half-graben (Manceda and Figueroa, 1995), one of the discrete depocenters resulting from the first rifting episode. In the study area, Early Jurassic marine deposits transgressed over diachronous and unfossiliferous fluvial conglomerates and sandstones (Rosenfeld and Volkheimer, 1981) of the El Freno Formation (Stipanicic

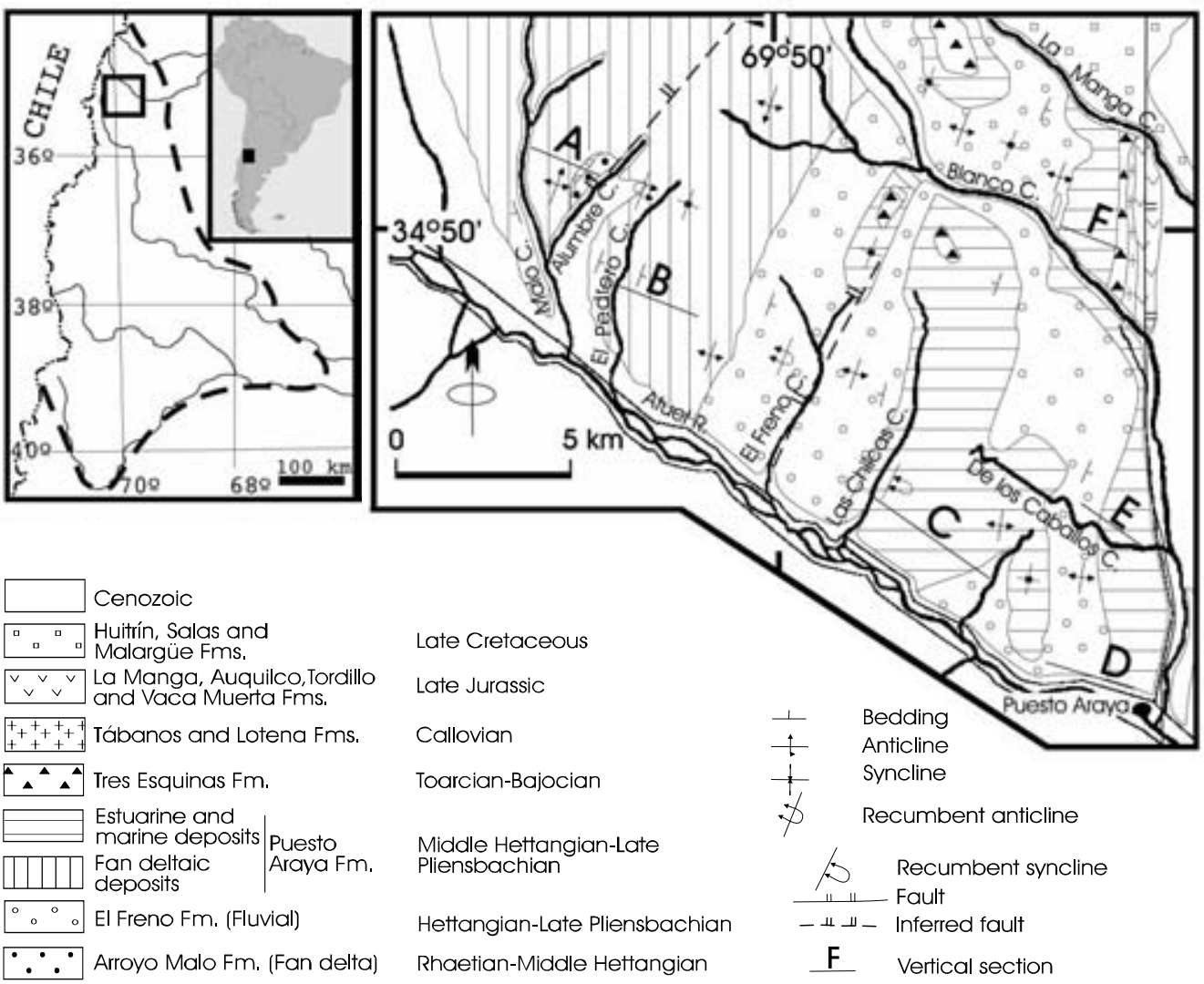

FIGURE 1 **Studied area at the northern Neuquén Basin showing the localities of the vertical sections. A: Arroyo Malo section; B: El Pedrero section; C: Las Chilcas section; D): Puesto Araya section; E: De los Caballos section; F: Codo del Blanco section.**

and Bonetti, 1970) whose base never crops out. The transgressive deposits are represented by two units: the Arroyo Malo Formation (Riccardi et al., 1997) of Rhaetian-Middle Hettangian age, which outcrops only in the Arroyo Malo creek (Fig. 1), and the Puesto Araya Formation (Volkheimer, 1978) of Middle Hettangian-Late Pliensbachian age, which covers a wider area.

Considering the transgressive deposits as a whole, the abrupt lateral changes of facies and age are remarkable (Reijenstein, 1967; Riccardi et al., 1988, 1991). Particularly, their base youngs toward the east from Rhaetian at Malo creek (Riccardi et al., 1997; Riccardi and Iglesia Llanos, 1999; Fig. 1) to Early Pliensbachian at Puesto Araya (Riccardi et al., 1988). Simultaneously, fine-grained marine sandstones and mudstones thin and the underlying fluvial conglomerates thicken and coarsen eastward. The Rhaetian age of the Arroyo Malo Fm. is the oldest record of the first transgression in the Neuquén basin.

METHODOLOGY

In order to interpret and discuss the tectosedimentary evolution of the Atuel valley during the Late Triassic-Early Jurassic and its likely structural controls, six vertical sections were chosen along two transverse east-west and north-south transects (Fig. 1) where lithofacies and taphofacies were analyzed and the depositional systems were determined. Sections were correlated based on ammonite, bivalve and brachiopod biostratigraphy. Sediment dispersal patterns and probable source areas (established according to the paleocurrents) together with biostratigraphical correlations and variation of maximum thickness allowed the paleogeographical features of the studied area to be inferred. Though a detailed explanation of

the facies analysis is beyond the scope of the present study, schematic vertical sections with facies association stacking patterns, tables with a general summary of the facies associations and photographs of some key lithofacies are given. Component lithofacies of the facies association can be verified in Tables 1 to 3 (in the Appendix). Facies association were named according to the dominant age of the deposits; T refers to those of Late Triassic-Middle Hettangian age and J refers to those of Middle Hettangian-Toarcian age. This criterion allows differentiating the facies associations of similar lithofacies compositions and different ages (see Tables 1 and 2).

Biostratigraphic correlation was based on ammonite, bivalve and brachiopod local zones of Riccardi et al. (2000). Two selected datums were used: *Epophioceras* Zone (Late Early Sinemurian-Late Sinemurian) at most of the sections and the *Tropidoceras* Zone to correlate Puesto Araya, Las Chilcas and De los Caballos sections (Fig. 2). All the localities show a good fossil record except the El Pedrero section which is almost unfossiliferous excluding its top, where *Weyla* sp. and *Gibbirhynchia derecki* allow it to be correlated to the top of Arroyo Malo section and the base of Las Chilcas, De los Caballos and Codo del Blanco sections, assigning them to the Late Early Sinemurian-Late Sinemurian. The correlation of El Pedrero and Arroyo Malo sections was done by consideration of the discontinuities and the lateral and vertical changes.

The age and areal distribution of the contemporaneous depositional systems allows identification of two regions in the Atuel valley, one to the east of El Freno creek and the other to the west (Figs. 1 and 2). Vertical sections of the western region (Arroyo Malo and El Pedrero sections, Figs. 3 to 5) are well bedded, coarsening- and thickening-upward mudstones, sandstones and conglomerates of Rhaetian-late Early Sinemurian age. Vertical sections of the eastern zone (Las Chilcas, Codo del Blanco, De los Caballos and Puesto Araya sections, Figs. 6 to 9) are well bedded, fining- and thining-upward sandstones and shales of late Early Sinemurian-Toarcian age. Extensive outcrops in both zones enable detailed facies analysis (Figs. 10 to 13).

RHAETIAN-LATE EARLY SINEMURIAN DEPOSITS

Deposits of Rhaetian-Late Early Sinemurian age only crop out in the western sections. Their base is unseen and the minimum thicknesses are 986 m and 633 m in Arroyo Malo (Figs. 3 and 4) and El Pedrero sections (Fig. 5), respectively. Both successions show massive mudstones or shales with sandstone interbeds, usually with slump folds or sedimentary faults. At the top of the Arroyo Malo section (Fig. 4) tangential cross-bedded sandstone and trough-cross bedded sandstone appear while massive and trough-cross bedded conglomerate and sandstone make up the top of El Pedrero section (Fig. 5).

In order to understand their paleoenvironmental evolution, these sections can be divided in three internal coarsening- and thickening-upward cycles (Fig. 2) of Rhaetian-Middle Hettangian, Middle Hettangian-middle Late Hettangian and middle Late Hettangian-late Early Sinemurian ages. The oldest cycle, 338 m thick, crops out only in the lower part of the Arroyo Malo section (Fig. 3). The Middle Hettangian-middle Late Hettangian cycle is 245 m and 196 m thick and middle Late Hettangian-late Early Sinemurian cycle is 403 m and 437 m thick in Arroyo Malo and El Pedrero sections, respectively (Figs. 4 and 5).

Facial stacking patterns of the cycles are very similar except for the youngest one whose deposits at the top of Arroyo Malo section differ from the rest. The stacking of facies associations are approximately T1-T2-T3-T4-T5 (Table 1, Fig. 3) for the Rhaetian-Middle Hettangian, J1-J2-J3 and J1-J2-J5 (Table 2, Figs. 4 and 5) for the Middle Hettangian-middle Late Hettangian cycle in Arroyo Malo and El Pedrero sections. These patterns show mudstone deposits and low-density turbidites at the base (Figs. 10A and 10B), high and low-density turbidites (Figs. 11C, 11E and 11F), slump-derived cohesive debris flows (Lowe, 1982) and sedimentary deformation (slumps, folds, faults, boudinage and load deformation among others, Figs. 3, 5, 10C, 11D and 11E) in the middle part. Slump-derived debris flows are represented as intraformational breccias with fragments of low-density turbidites (Fig. 10D). The stacking patterns end with channelized hyperconcentrated flow deposits, high and low density turbidites and traction current deposits (FiG. 10F) encased into interchannel areas of low and high-density turbidites and mudstones. A remarkable trend of these patterns is an upward increase of debris flow deposits, hyperconcentrated flow deposits, traction current deposits and an upward widening of the lenses of trough-cross bedded sandstones.

The middle Late Hettangian-late Early Sinemurian cycle lacks the finest levels and its facies stacking pattern is J2-J5-J6 and J2-J3-J4 (Table 2) in Arroyo Malo and El Pedrero sections, respectively (Figs. 4 and 5). Its base includes low and high-density turbidites and slump-derived debris flow deposits with sedimentary deformation. As above, these stacking patterns show an upward increase of debris flow deposits, hyperconcentrated flow deposits, lensoidal traction current deposits and an upward widening of the lenses of trough-cross bedded sandstones and conglomerates which are well developed at the top of the El Pedrero section (J6 in Table 2, Fig. 5)

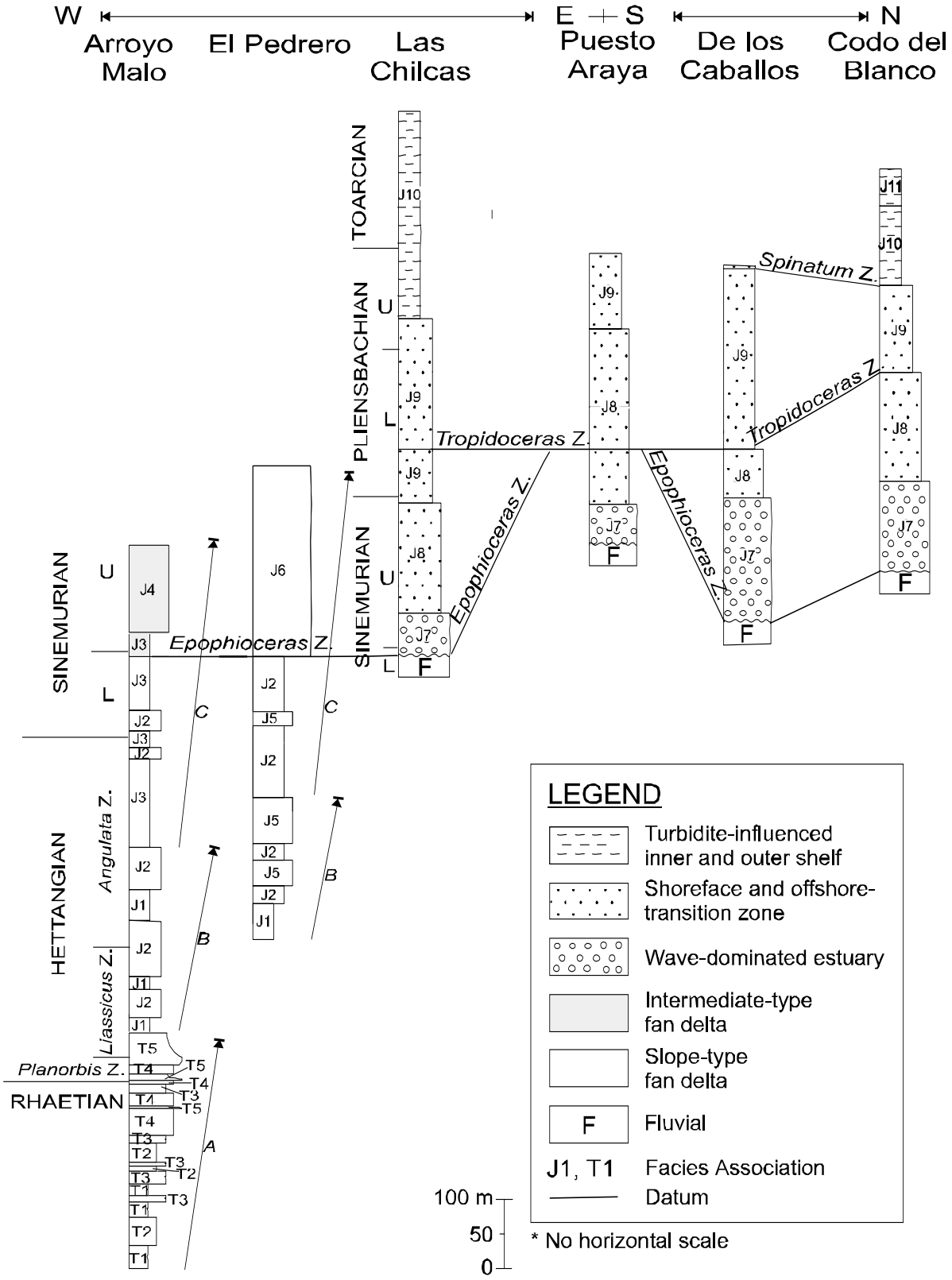

FIGURE 2 **Biostratigraphic correlation of the studied vertical sections. Stage divisions are shown except for the Hettangian whose ammonite standard zones are present. Datums are based on the ammonite zonation for the Neuquén basin (Riccardi et al., 2000). Only the vertical thickness of the Puesto Araya section is out from scale due to problems of drawing. Vertical arrows mark the shallowing-upward fan delta cycles. A: Rhaetian-Middle Hettangian cycle (vertical section in Fig. 3); B): Middle Hettangian-middle Late Hettangian cycle; C: middle Late Hettangian-late Early Sinemurian cycle (vertical sections in Figs. 4 and 5).**

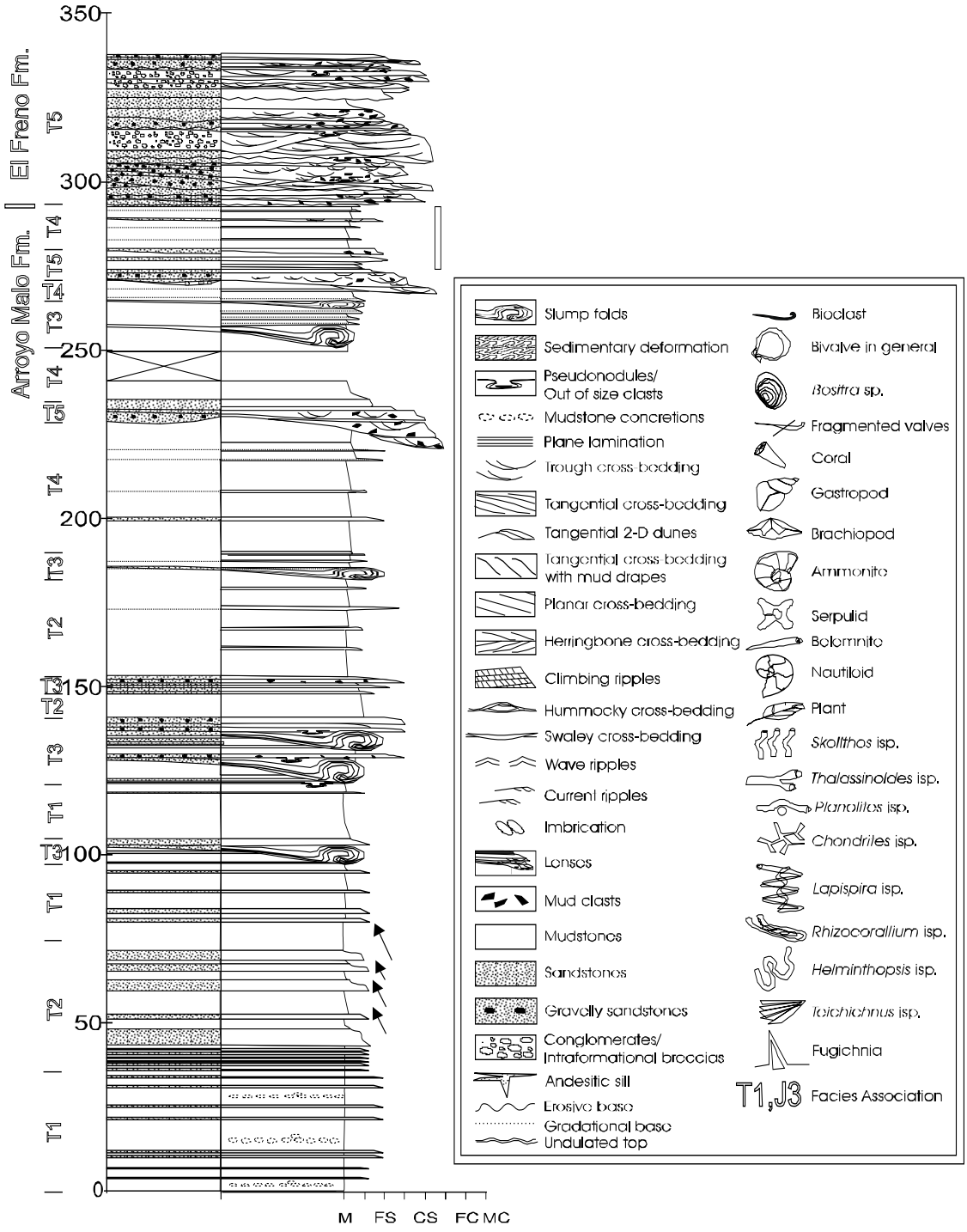

FIGURE 3 | **Simplified vertical section of the Late Triassic-Middle Hettangian cycle at the base of the Arroyo Malo section. Small arrows: small-scale fining- and thinning upward units also illustrated in Fig. 10E. Vertical bar refers to the interval showed in Fig. 10E.**

where they represent distributary channels and chutes. At the top of the Arroyo Malo section these upper deposits are replaced with tangential cross-bedded sandstones with sets 0,5 to 5 m thick (Fig. 5, and J4 in Fig. 11G) cut by channelized trough-cross bedded sandstones interpreted as mouth bars cut by distributary channels (J4, Table 2) of late Early Sinemurian age.

Excluding the deposits of the top of the Arroyo Malo section (J4, Table 2), each coarsening- and thickening-upward cycle is interpreted as a shallowing-upward fluviodominated slope-type fan delta in a marine basin, below wave base according to the stenohaline fossils and the absence of wave structures. Basin plain and fan deltaic prodeltas, lower fronts and upper fronts are recorded.

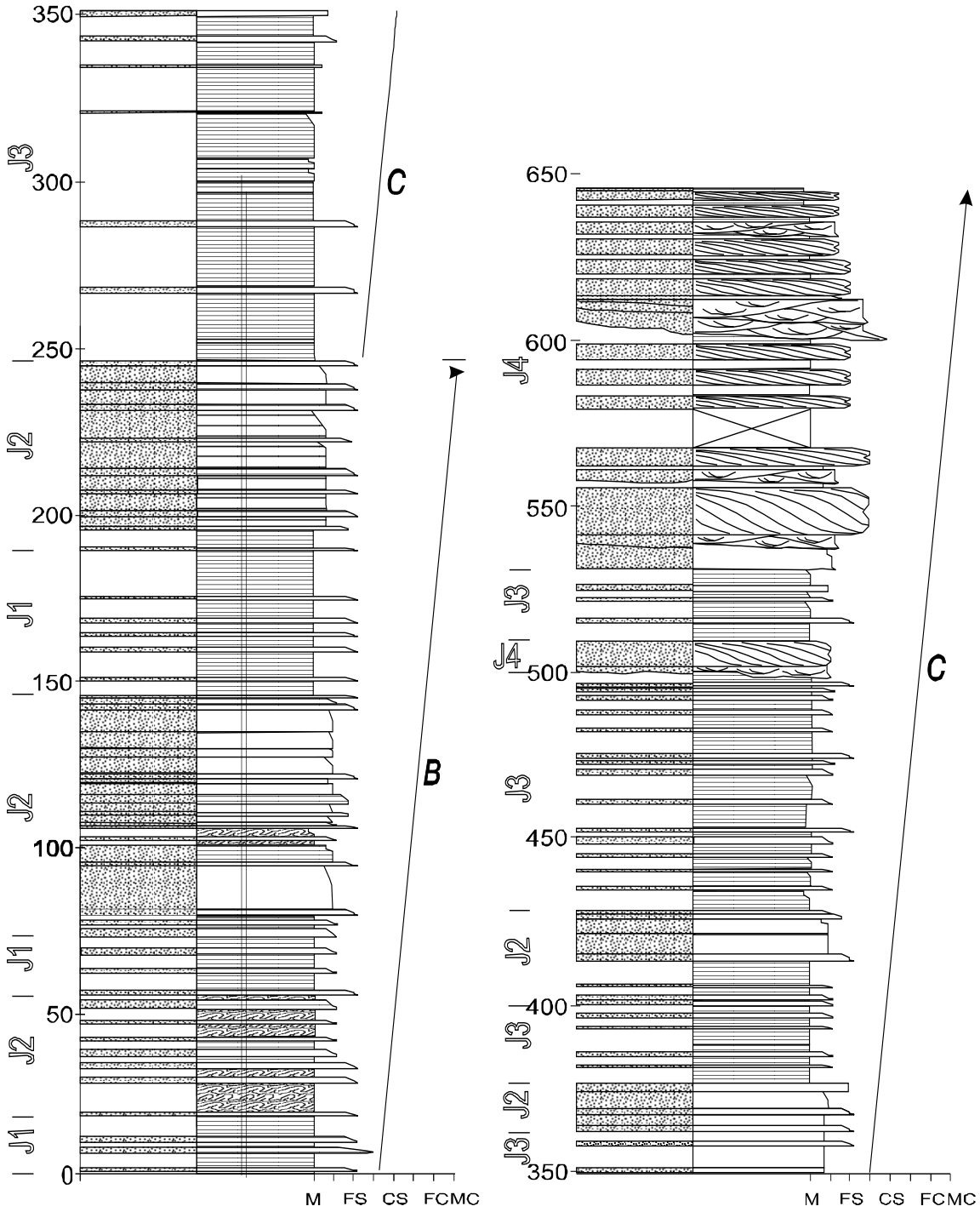

FIGURE 4 | **Simplified vertical section of the Middle Hettangian-middle Late Hettangian (B arrow) and middle Late Hettangian-late Early Sinemurian cycles (C arrow) of the Arroyo Malo section.**

Fan deltas were first defined as alluvial fans prograding into a lake or marine basin (Holmes, 1965) and since 1988 they are considered as subaqueous sedimentary prisms deposited by active alluvial fans in the basin-alluvial fan interface (Nemec and Steel, 1988). Fan deltas are related to high source areas and slopes (Nemec and Steel, 1988; Prior and Bornhold, 1989; Reading and Collinson, 1996; Postma, 1990a) and particularly the slope-type fan deltas (Ethridge and Wescott, 1984) have a slope or steep front connected downward to a turbiditic prodelta. First this slope was the continental rise (Ethridge and Wescott, 1984) but afterward it included any structural (Surlyk, 1984; Colella, 1988a; Orton, 1988, Gloppen and Steel, 1981;

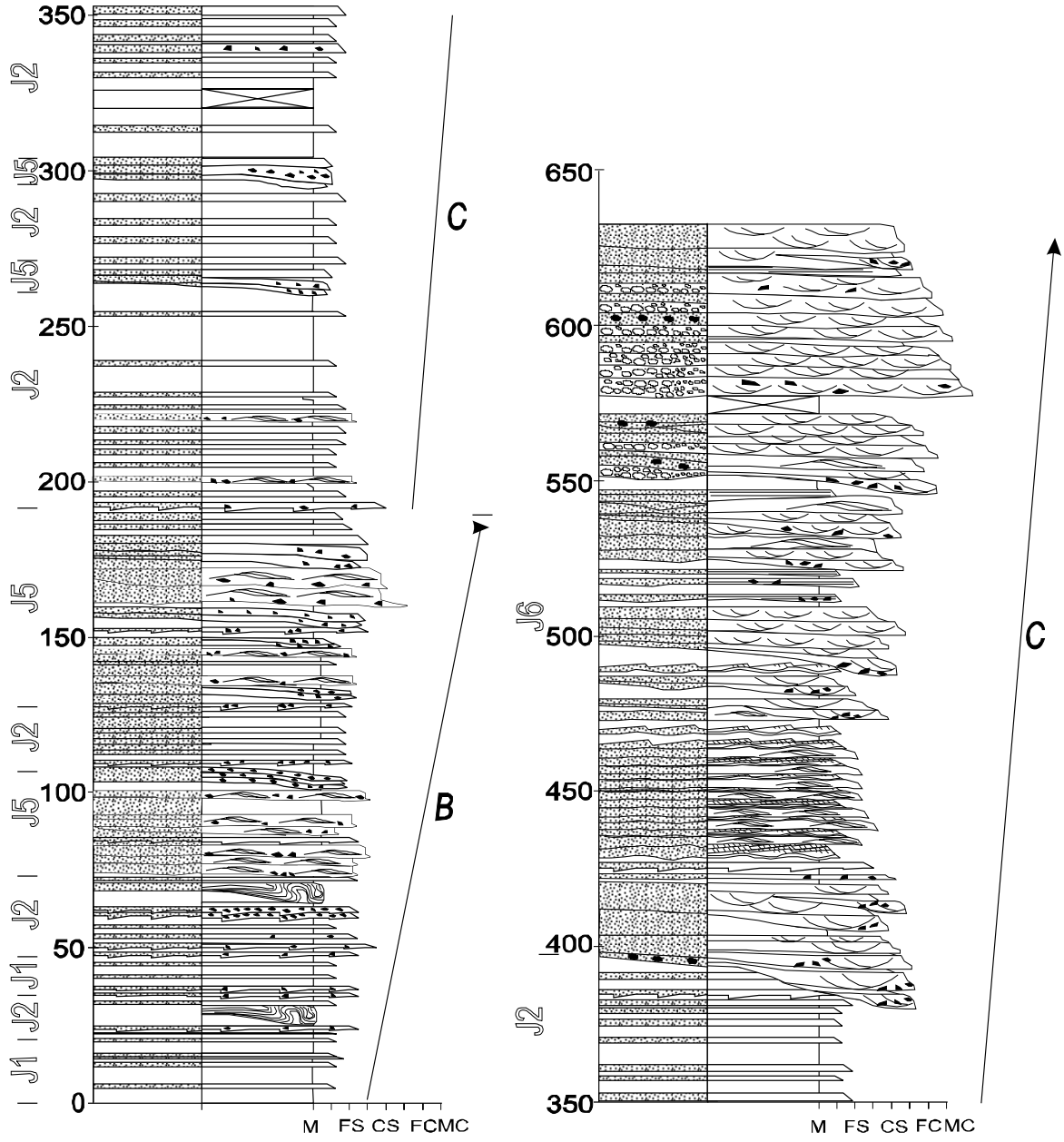

FIGURE 5 | **Simplified vertical section of the Middle Hettangian-middle Late Hettangian (B arrow) and middle Late Hettangian-late Early Sinemurian cycles (C arrow) of the El Pedrero section.**

Steel, 1988; Massari and Colella, 1988; Postma, 1990b) or erosive (Prior and Bornhold, 1989, 1990; Bornhold and Prior, 1990; Nemec and Steel, 1988; Postma, 1990b) slope. Turbiditic prodelta deposits of the slope-type fan deltas result from hyperpycnal flows with sediment concentration high enough to generate turbidity currents at the fluvial mouths (Prior et al., 1987; Normark and Piper, 1991; Mulder and Syvitski, 1995; Mulder et al., 1998; Balance, 1988; Wheatcroft et al., 1997).

At the Arroyo Malo and El Pedrero sections, the slumps, slump folds, turbiditic prodelta, paleoslopes, paleocurrents and the absence of tidal or wave structures allow three stacked transverse fluviodominated slope-type fan deltas to be inferred. The paleotectonic framework of the studied area, located in the Atuel-Valenciana half-graben, suggests that the slopes were controlled by normal faults. Rhaetian-Middle Hettangian slope-type fan delta was controlled by a normal fault located at the present Alumbre creek (Fig. 1) while the slope-type fan deltas of Middle Hettangian-middle Late Hettangian and middle Late Hettangian-late Early Sinemurian ages were controlled by a fault located at the El Freno creek (Fig. 1). Along the studied successions fan delta paleoslopes

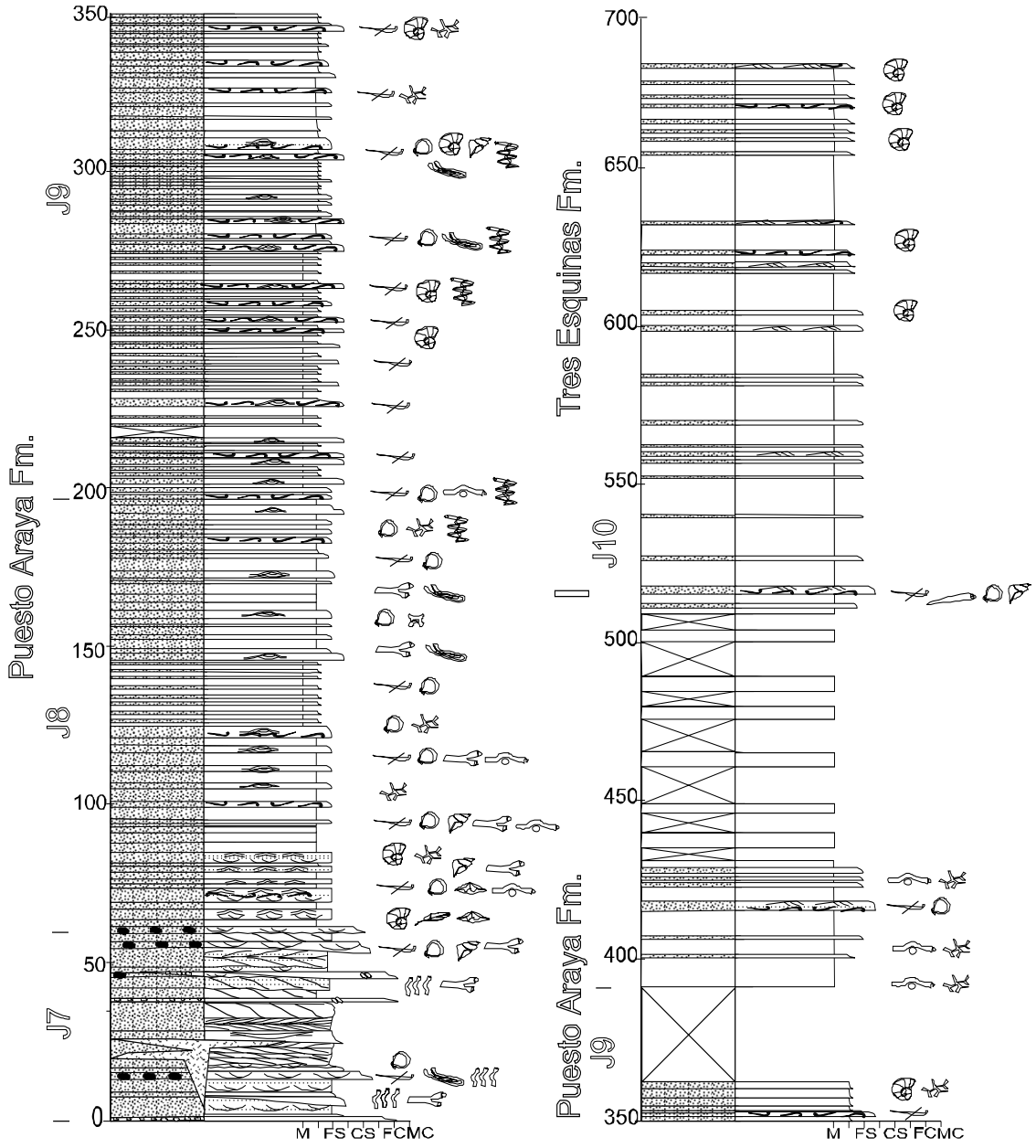

FIGURE 6 **Simplified vertical section of the late Early Sinemurian-Toarcian cycle in Las Chilcas section.**

varies from WSW to NW (Az 260º to 330º) while most paleocurrents range from SSW to NW (Az 190º to 335º; Lanés, 2002).

The top deposits of the Arroyo Malo section, considered mouth bars (Fig. 4, J4 in Fig. 11G, and Table 2) do not fit in the interpretation of slope-type fan deltas. Their geometry, showing one set of cross-bedded sandstones are reminesent of thin foresets of the Gilbert-type fan deltas (Ethridge and Wescott, 1984). Foreset thickness of the Gilbert-type fan deltas ranges from 3 to 8 m (Kazanci, 1990) up to several tens of meters thick. The low thickness of the mouth bars at the top of the Arroyo Malo section and the lack of gravity deposits in their foresets differ from the real Gilbert-type fan deltas. Mouth bars can be deposited in shallow basins with less than 3º dip (Orton, 1988; Postma, 1990b) which allow the friction of the effluents against the bottom (Kleinspehn et al., 1984; Massari and Colella, 1988; Reading and Collinson, 1996). In a faulted-block topography such conditions control the sedimentation in the gentle sloping areas of the hanging wall just opposite to the main fault (Gloppen and Steel, 1981; Massari and Colella, 1988; Gawthorpe

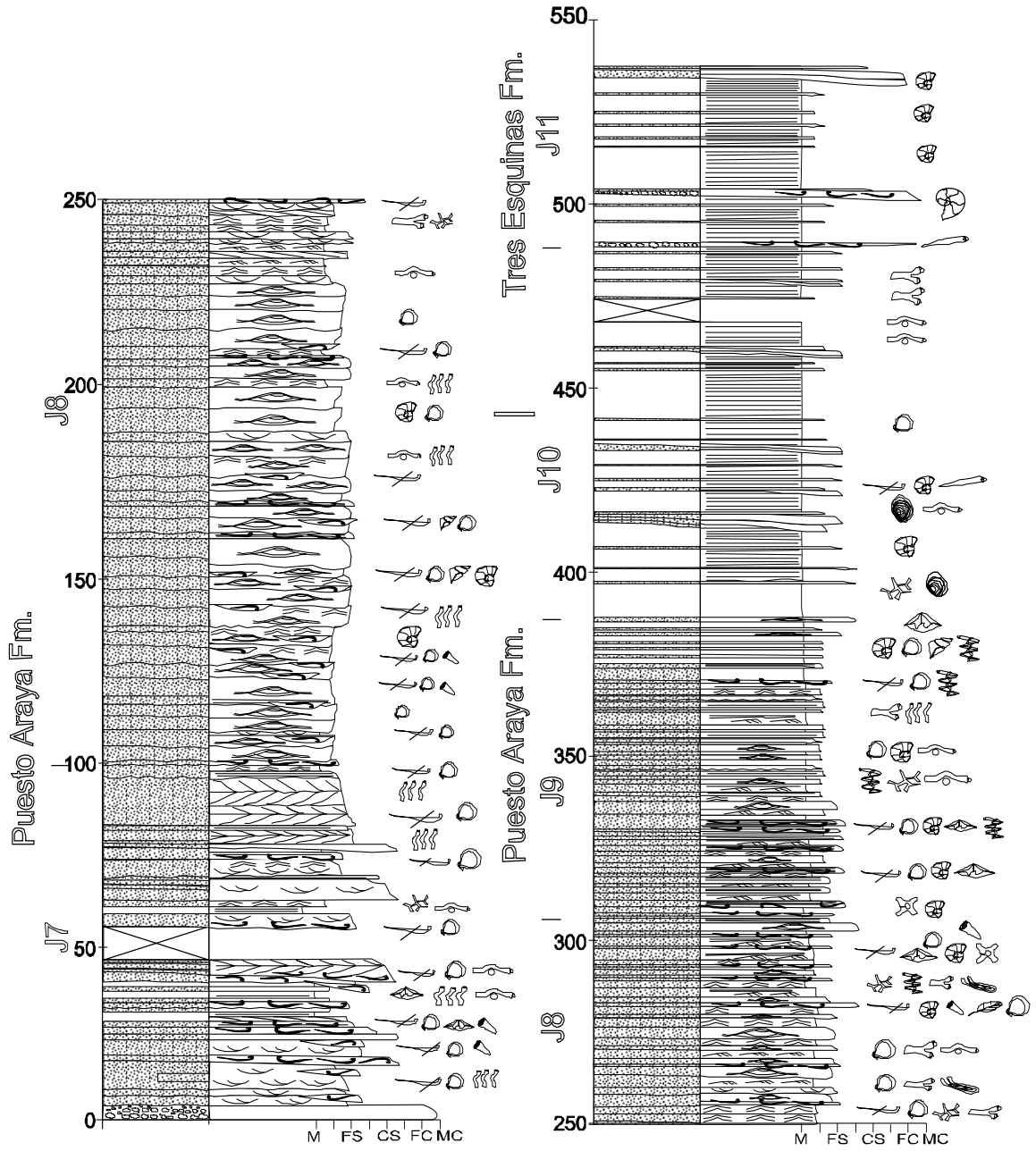

FIGURE 7 **Simplified vertical section of the late Early Sinemurian-Toarcian cycle in Codo del Blanco section.**

and Colella, 1988; Colella, 1988b). The low dip above contrasts with the dips higher than 15º (Prior and Bornhold, 1990) or between 12° and 16° (Prior et al., 1981; Kostaschuk and McCann, 1987) required for slumping or chute incision in the slope-type fan deltas. The mouth bar deposits without wave evidence lead us to consider the fan delta of the top of Arroyo Malo section as an intermediate shelf to Gilbert-type fan. Then the slope-type fan delta of middle Late Hettangian-middle Early Sinemurian age changed to an intermediate shelf to Gilbert-type fan during the late Early Sinemurian.

LATE EARLY SINEMURIAN-TOARCIAN DEPOSITS

Deposits of late Early Sinemurian-Toarcian age crop out in Las Chilcas, De los Caballos, Codo del Blanco and Puesto Araya sections (Figs. 1, 2, 6, 7, 8 and 9) overlying fluvial conglomerates and sandstones. They are well bedded, fining- and thinning-upward sandstones and shales, 685 m thick (Las Chilcas section), 538 m (Codo del Blanco section), 490 m (De los Caballos section) and 496 m (Puesto Araya section).

The vertical stacking pattern of facies associations is J7-J8-J9-J10-J11 (Table 3) though the details of facies

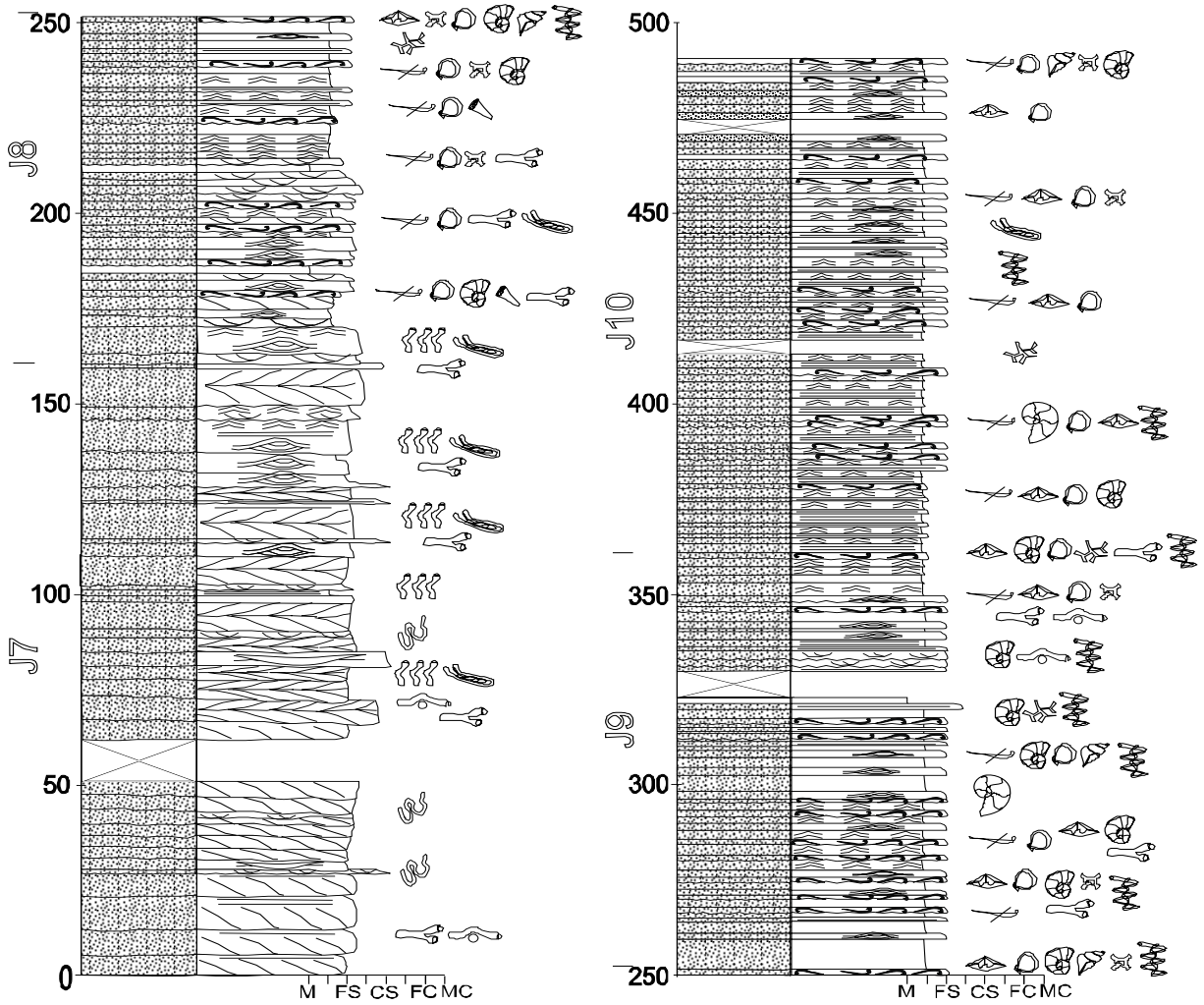

FIGURE 8 | **Simplified vertical section of the late Early Sinemurian-Toarcian cycle in De los Caballos section.**

composition show slight differences according to locality. Las Chilcas, De los Caballos and Puesto Araya sections (Figs. 6, 8 and 9) show shallow subtidal to intertidal deposits of tidal inlets and tidal sandwaves (J7 in Table 3, and Fig. 11) at the base. These basal deposits interfinger with storm and fair-weather wave and current deposits at De los Caballos section and with mudstones from the central estuary and washover fan deposits at Codo del Blanco section that confirm an outer estuary setting. Amalgamated and non-amalgamated storm and fair-weather wave and current deposits crop out (J8 and J9 in Table 3, and Fig. 13) in the middle sections. The top deposits, represented by shales, low-density and high-density turbidites and some hyperconcentrated flow deposits, appear only at the top of Las Chilcas and Codo del Blanco sections (J10 and J11 in Table 3, and Figs. 6 and 7). In every locality a fining- and thinning-upward trend together with a decreasing-upwards faunal diversity and benthos were observed, suggesting decreasing oxygen levels of interstitial waters.

Eastern successions resulted from the transgression of a storm-dominated shelf with sedimentary paleoenvironment evolving from a wave-dominated estuary (cf. Reinson, 1992; Dalrymple et al., 1992) to a turbidite-influenced outer shelf. The storm-dominated shoreface, offshore to shoreface transition zone and an inner-shelf influenced by low-density and high-density turbidity currents were recorded.

Paleocurrents evidence a NNE-SSW to NE-SW (Az 35°-215° to Az 42°-222°) paleoshoreline of the wave-dominated estuary and a NNW to NE (Az 350°-170° to Az 240°-60°) paleoshoreline of the storm-dominated shelf. The difference between them is likely related to the coast straightness due to the sandstone deposition of the outer estuary.

The high textural maturity of the tidal inlet conglomerates (Figs. 12B and 12C) together with a lithological composition similar to the underlying fluvial conglomerates evi-

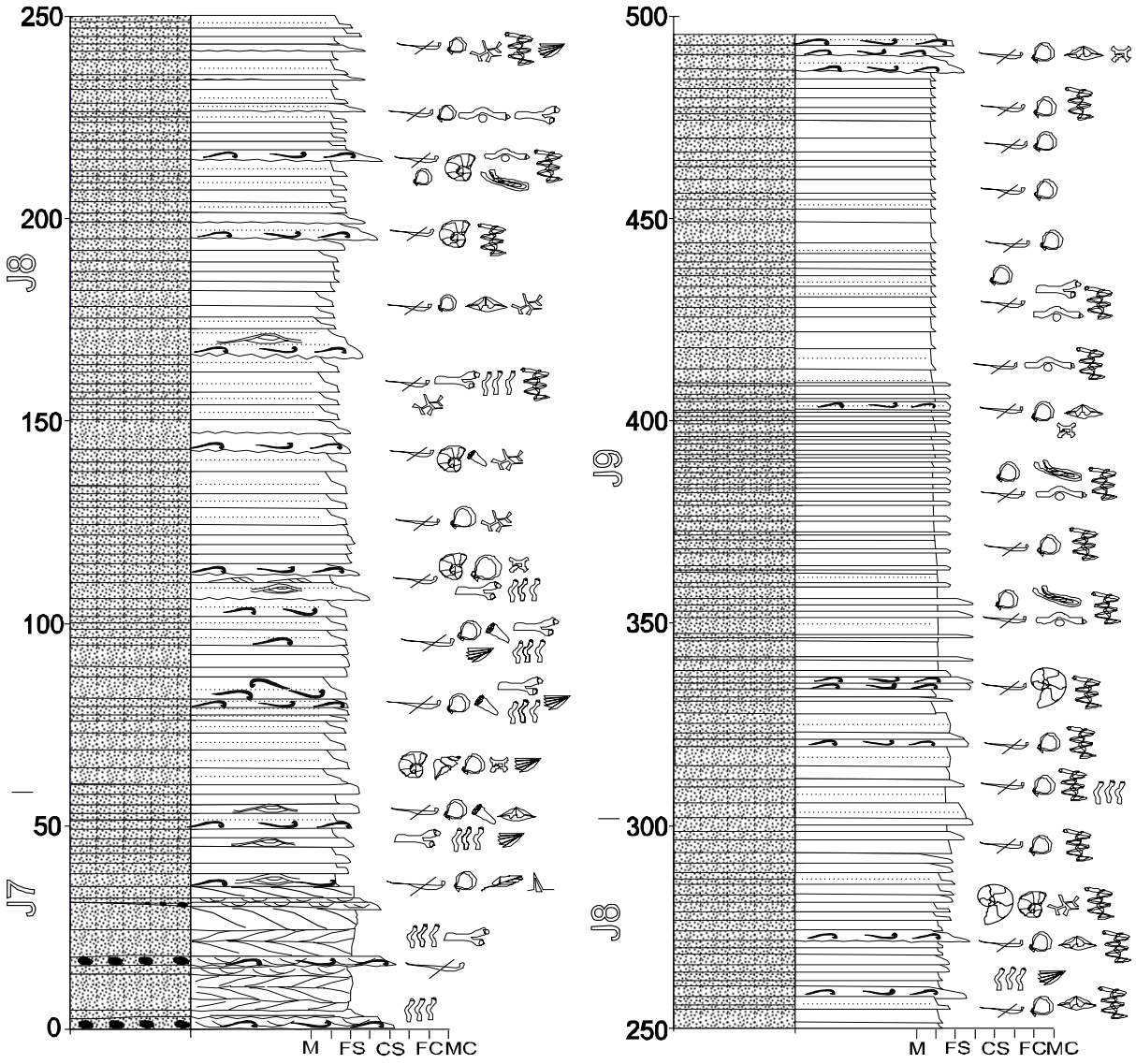

FIGURE 9 | **Simplified vertical log of the Puesto Araya section (Early Pliensbachian-Late Pliensbachian).**

dence an extended reworking of the fluvial deposits above fair-weather wave base, as the transported freshwater bivalves (*Cardinioides* n. sp., Damborenea, pers. comm.) from the tidal inlet deposits confirm. High textural and compositional maturity of the estuary sandstones, very different from the fluvial ones, also indicate the reworking above fair-weather wave base, typical from the wave and storm-dominated foreshores (Leithold and Bourgeois, 1984).

Monospecific pavements of *Bositra* sp. in laminated shales at the top of Codo del Blanco section (Fig. 7), together with calcareous nannofossils (*Ellipsagellosphaera britannica* and *Crepidolithus* sp.) and ammonites from the *Spinatum* Zone evidence short events of dysaerobic (O_2<0,6 ml O_2/l of H_2O; Brett and Baird, 1986) bottom waters in an anaerobic (O_2<0,1 ml O_2/l of H_2O; Brett and Baird, 1986) inner shelf by the end of the Pliensbachian.

PALEOENVIRONMENTAL AND PALEOTECTONIC EVOLUTION

Some useful criteria to interpret the evolution of depositional systems and their controlling factors directly derive from the vertical stacking patterns. The controlling factors include the accommodation, accommodation vs. sedimentary supply ratio and creation of accommodation rate. Accommodation is the available space for sedimentation at certain place and time (Jervey, 1988). It mainly depends on subsidence, sedimentary supply and eustatic changes (Posamentier and Allen, 1993a, 1993b; Steckler et al., 1993; Gawthorpe et al., 1993; Howell and Flint, 1996) that determine the features and distribution of the depositional systems. A sediment supply greater than the accommodation (supply >> accommodation) produces prograding coarsening- and thickening-upward deposits, usually showing a sigmoidal geometry in a 2-D cross sec-

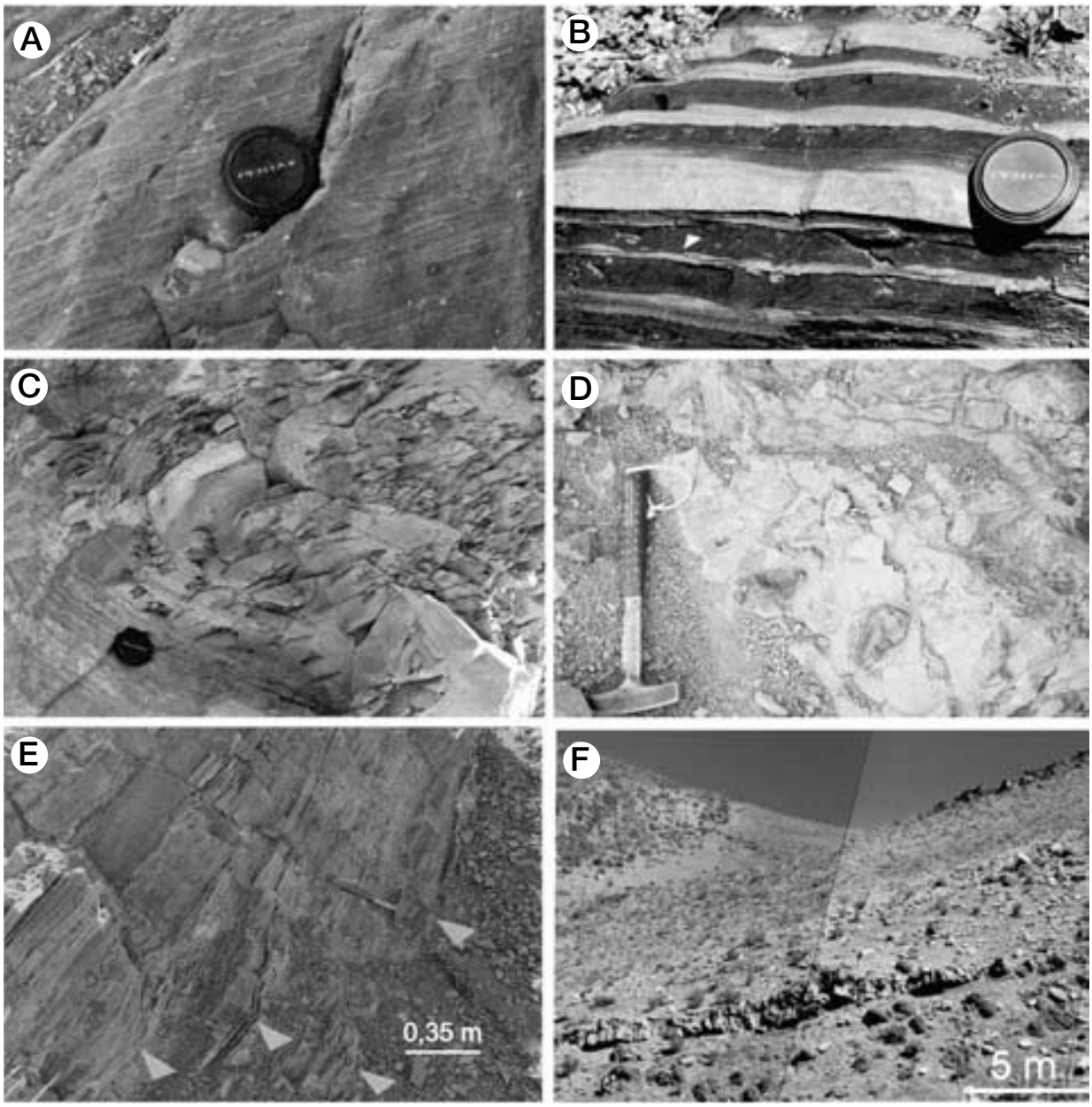

FIGURE 10| **T1, T2, T3, T4 and T5 facies associations. A) Td-e turbidites with out sized clasts. Lens cap diameter 6 cm. B) Tc-e turbidites. Triangle points to micro-climbing ripples. Lens cap diameter 6 cm. C) Slump fold in a low-density turbidite succession. Lens cap diameter 6 cm. D) Intraformational breccia with fragments of low-density turbidites. Compare the clasts to the turbidites in A and B. Hammer length 35 cm. E) Lensoidal small-scale fining- and thinning upward units showed by the vertical bar in Fig. 3. Triangles point to the bases of the lenses. F) T5 facies association. Lenses of trough-cross bedded sandstones encased into low and high-density turbidites of the in interchannel areas.**

tion. An accommodation exceeding the sediment supply (accommodation >> supply) produces retrograding fining- and thinning-upward successions.

Another accommodation-related concept is the relative sea-level change, directly interpreted from the sedimentary successions without considering any posible tectonic or eustatic influence on the sea-level change. Then a prograding coarsening- and thickening-upward succession implies a relative sea-level fall while a retrograding fining- and thinning-upward one evidences a relative sea-level rise. Considering the relative sea-level allows a first approach to the inferred sea-level changes without tectonic or eustatic implications, which can be lately evaluated. In order to identify such implications in the Rhaetian-Toarcian sea-level changes, the evolution of the studied successions was contrasted with the global eustatic sea-level chart (Haq et al., 1987) and the tectonic evolution of the Neuquén Basin (Vergani et al., 1995). It must be noted that the only published tectonic evolution of the Neuquén

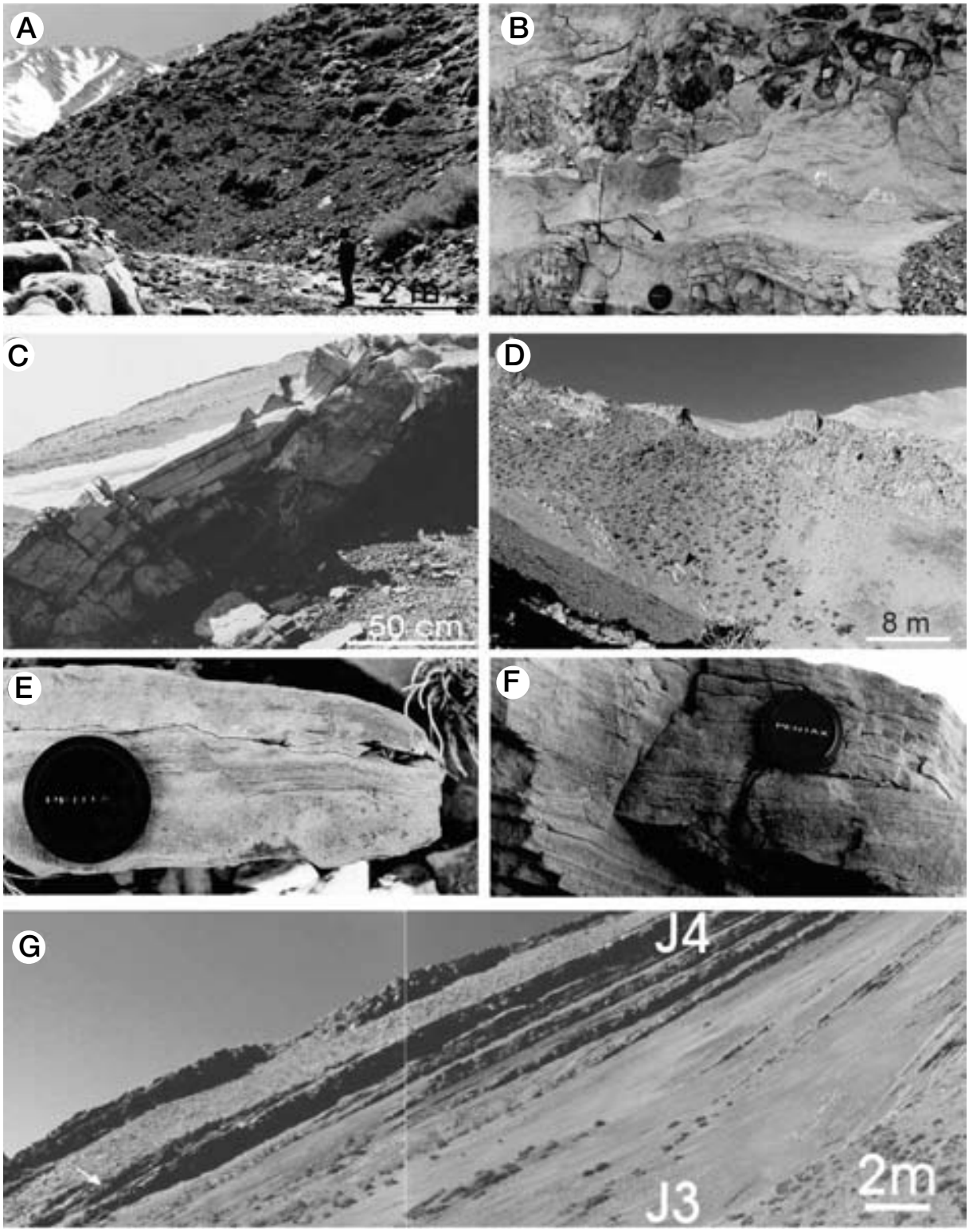

FIGURE 11 **J1, J2, J3, J4, J5 and J6 facies associations. A) General aspect of the deposits of the J1 facies association in the base of El Pedrero section. B) Ta turbidite deposits with mud blocks and deformed base by injection of underlying sediment. The arrow points an isolated tangential 2-D of a high-density turbidite. Lens cap diameter 6 cm. C) Isolated tangential 2-D in a high-density turbidity current deposit after a hydraulic jump. D) Slump folds (triangle) in deposits of J2 facies association at Arroyo Malo section. E) Small sedimentary fault in a Ta-c turbidite. Lens cap diameter 6 cm. F) Fluid escape structures in Tb-e turbidites. Lens cap diameter 6 cm. G) Mouth bar deposits (J4) at the top of Arroyo Malo section, overlying massive pebbly mudstones and low density turbidites (J3) from the fan delta lower front. The arrow points to a foreset surface of the tangential cross bedding.**

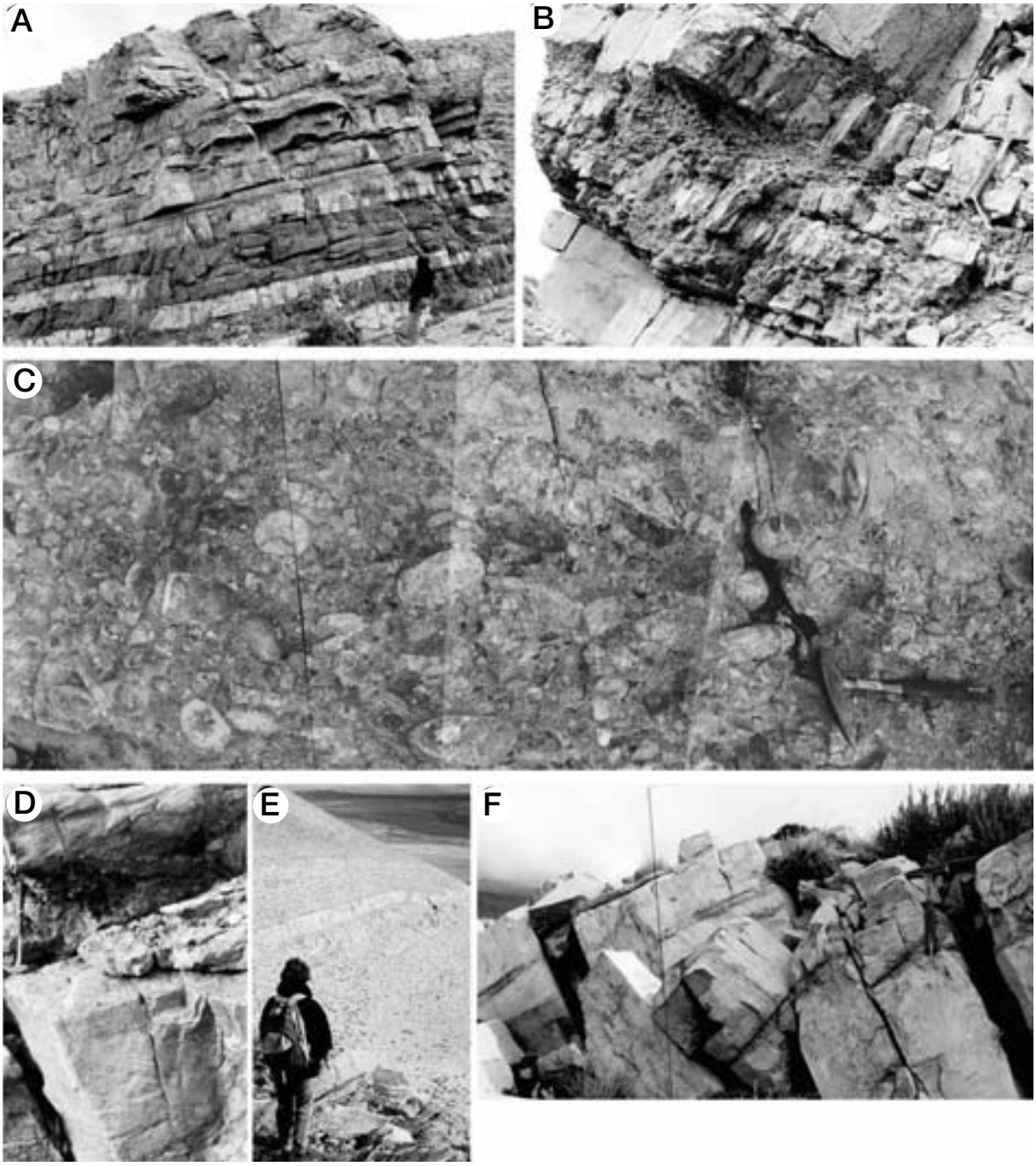

FIGURE 12| **J7 facies association. A) General aspect of the estuarine deposits at the base of Las Chilcas section, intruded by andesite sills (dark grey) (see Fig. 6). The arrow points to the base of a conglomeratic tidal inlet deposit. Person 1,60m. B) Cross-section of the multiepisodic conglomeratic tidal inlet deposit shown in B. Each episode deposit shows a basal normal graded clast-supported conglomerate and a trough-cross sandstone at the top. Hammer length 35 cm. C) Detailed of the structure of the conglomeratic tidal inlet deposits at Codo del Blanco section. Note the imbrication in opposite directions. Hammer length 35 cm. D) Herringbone-cross bedding. Hammer length 35 cm. E) General aspects of the estuarine deposits at the base of Puesto Araya section. The arrow marks a foreset surface of a tidal sandwave. View on flow-parallel direction. Person 1,60 m. F) Low preservated tidal sand wave deposit with thick mud drapes (dark grey). Hammer length 35 cm.**

Basin is based on data from its southern part, different from the northern basin where the study area is located.

As mentioned above, the fan delta successions of the studied area can be divided into three coarsening- and thickening upward cycles. Inside these cycles, a series of fining- and thinning-upward units of minor scale can be observed (see the small arrows in Fig. 3 and Fig. 10E). These coarsening- and thickening upward cycles are interpreted as resulting from lowstand and the consequent

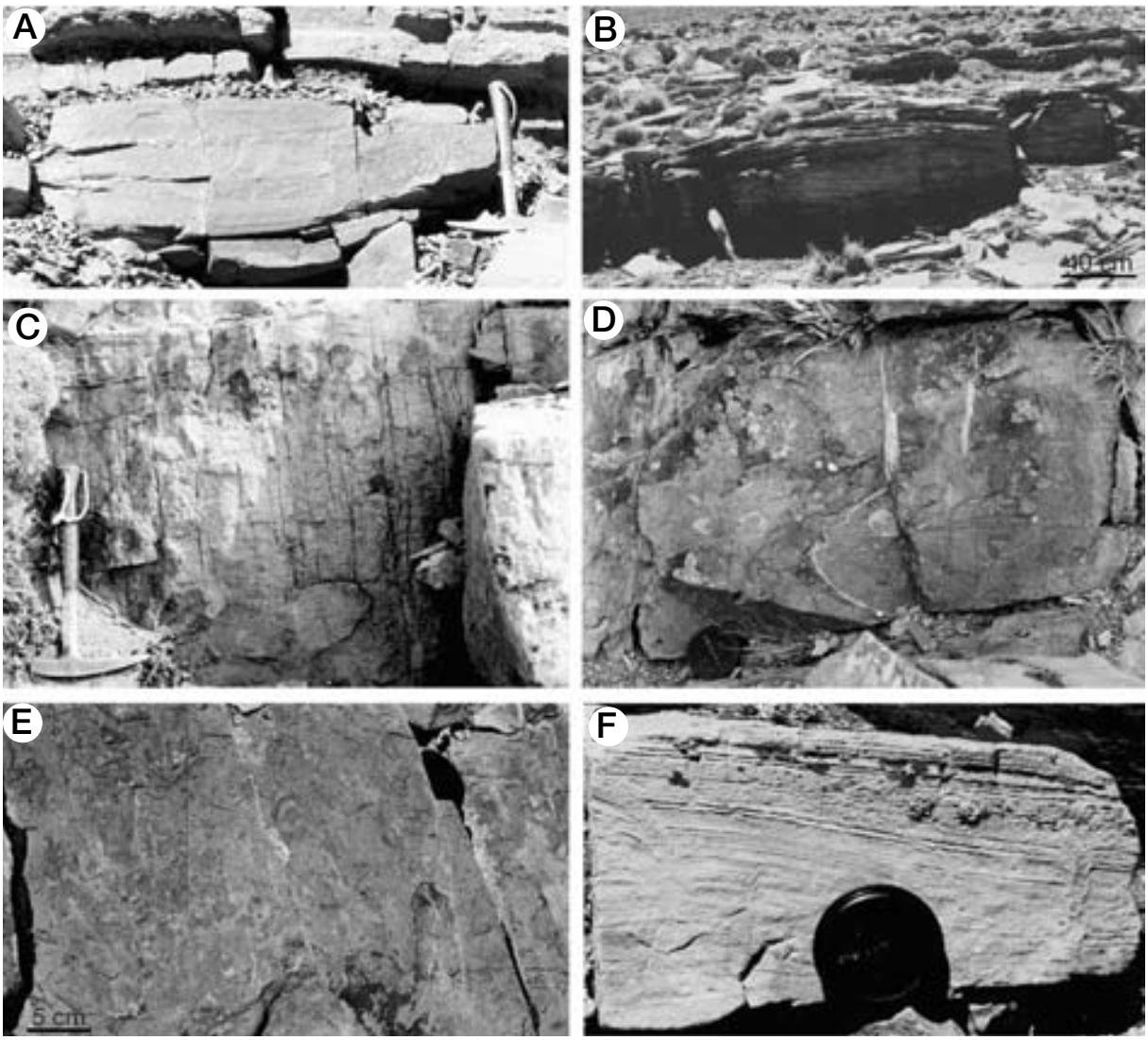

FIGURE 13 **J8 and J9 facies association. A) Isolated swale from a swaley-cross stratified bed. Hammer length 35 cm. B) Hummocky-cross bedding. C) Piperock in a trough-cross bedded sandstone with a wave-rippled top. Hammer length 35 cm. D) Massive shelly tempestite with solitary corals of rounded cross-sections. A big-size edgewise disarticulated bivalve can be seen. Lens cap diameter 6 cm. E) Massive shelly tempestite with numerous disarticulated and fragmented bivalves. F) Fugichnia in a hummocky-cross stratified tempestite of the J9 facies association. Lens cap diameter 6 cm.**

fan delta forestepping, which is the deposition of shallow facies in deep basin areas. Consider a slope-type fan delta located in a coastal mountain range, connected downslope to a narrow shelf, slope and basin plain. During a lowstand, the sediment would bypass the shelf and slope to be deposited straight in the basin plain (Mutti, 1992) in a process known as forestepping. When the sea level slowly rises again and shelf accommodation increases, the sediment would be deposited close to the slope or directly over the shelf. At the highstand and maximum accommodation on the shelf, the sediment would be retained in the mountain range and the supply to the basin and shelf would decrease to a minimum. The record of the complete shallowing-deepening events described above, deposited during a complete eustatic cycle from lowstand to highstand, is fining and thinning-upward (Fig. 3; Mutti, 1992; Muto, 1993; Mutti et al., 1996, 1999) due to the deposition of retrograding slumps and, subaqueous flows of decreasing volume. Only the basal part of these complete events, produced by the forestepping, can be coarsening- and thickening upward due to the increasing sedimentation of high-density gravity flows of the forestepping. (In this case the complete lowstand to highstand eustatic cycle is reflected by a succession which is firstly coarsening- and thickening upward and then fining- and thinning-upward).

Both progradation and forestepping result in the deposition of shallow facies over deep ones. However the progradation depends on a sedimentary supply greater than the accommodation and it produces sigmoidal fan deltas (e.g. Gilbert-type fan deltas) whose

geometry evidence a fairly steady supply. On the contrary, the forestepping is related to tectonic uplift of the source area and a flashy sediment supply, which impede the organization of sigmoidal deposits. The lowstand responsible for the fan delta forestepping can be caused by eustatic sea level lowstands (Field et al., 1999; Rasmussen, 1997); tectonic uplift and consequent lowering of the source area (Mutti, 1992; Mutti et al., 1996, 1999; Muto, 1993; Gloppen and Steel, 1981; Surlyk, 1984; Dabrio, 1988; Mastalerz, 1995; Chough and Hwang, 1997; Chansong et al., 2001) and increased rainfalls in the source area or flashy floods which originate hyperpycnal flows at fluvial mouths (Mutti et al., 1996; Dam and Surlyk, 1992; Mulder and Syvitski, 1995; Soh et al., 1995; Weinrich, 1989).

The small fining- and thinning-upward units (see the small arrows in Figs. 3 and 10E) inside the coarsening- and thickening upward cycles reflect the deposition of retrograding slumps and subaqueous flows of decreasing volume (Mutti, 1992; Muto, 1993; Mutti et al., 1996, 1999) after a flashy sediment supply, which usually controls the sedimentation of slope-type fan deltas related to braided alluvial systems. The small fining- and thinning-upward units in the studied fan deltaic successions reflect flashy floods or increased rainfalls in the source area and the formation of hyperpycnal flows at fluvial mouths (Mutti et al., 1996; Dam and Surlyk, 1992; Mulder and Syvitski, 1995; Soh et al., 1995; Weinrich, 1989).

In summary, the three coarsening- and thickening upward cycles of the studied fan deltaic successions are interpreted as resulting from lowstand and the consequent fan delta forestepping occurred at Middle Hettangian, middle Late Hettangian and late Early Sinemurian. The small-scale fining- and thinning-upward units inside the cycles reflect the flashy sediment supply, which controlled the fan deltaic sedimentation up to late Early Sinemurian.

Despite the similar age of the top deposits of Arroyo Malo and El Pedrero sections they belong to different depositional systems according to their vertical stacking patterns and interpretation. Top deposits at El Pedrero section (Fig. 5) are interpreted as a part of a slope-type fan delta upper front while the prograding deposits of the top of Arroyo Malo section (Fig. 4 and J4 in Fig. 11G,) belong to an intermediate shelf to Gilbert-type fan delta. Slope-type fan deltas are related to steep slopes, relatively deep basins and an accommodation greater than supply (accommodation >> supply); being usual during synrift phases (Prior and Bornhold, 1990; Colella, 1988b; Massari and Colella, 1988). Slope-type fan delta dominated the Arroyo Malo and El Pedrero sections up to the late Early Sinemurian, showing a strong aggradation (aggradation >> progradation), an accommodation greater than sedimentary supply (accommodation >> supply) and a high creation of accommodation rate. On the contrary the intermediate fan delta with mouth bars of the top of Arroyo Malo section is strongly prograding (aggradation << progradation) and it is an evidence of a shallow and low gradient basin, a supply greater than accommodation (accommodation << supply) and a low creation of accommodation rate. The decrease of accommodation occurred during the late Early Sinemurian.

Studied fan delta successions record several forestepping events or relative lowstands at Middle Hettangian, middle Late Hettangian and late Early Sinemurian (Figs. 3 to 5). If one considers the change of the petrographic composition of the underlying and overlying units as a criterion to identify a sequence boundary (Emery and Myers, 1996), the absence of muscovite in the Middle Hettangian shales compared to the underlaying Rhaetian ones suggests a lowstand at Middle Hettangian. The fragments of marine shell beds and storm beds as clasts in the upper conglomerates of El Pedrero section evidence the erosion of the marine shelf during the late Early Sinemurian. The fault at Alumbre creek seems to have stopped its activity after the Middle Hettangian because no younger sedimentary reactivations are observed in the Arroyo Malo section (Figs. 2 to 4) (Lanés, 2002). The forestepping records above were compared to the Jurassic global eustatic curve (Haq et al., 1988) in order to determine their tectonic, eustatic or climatic controlling factors. The three forestepping events coincide with lowstands of the short term eustatic curve (Haq et al., 1987). On the other hand, the forestepping records are similar to the hangingwall sequences of normal faults (Howell and Flint, 1996; Gawthorpe et al., 1993) and fining-upward/coarsening-upward units from rifts (Ravnås and Steel, 1998). Considering the paleostructural framework of the study area and the similarities above, Middle Hettangian forestepping could have resulted from the activity of the fault at the Alumbre creek (Fig. 1) while the middle Late Hettangian and late Early Sinemurian foresteppings could have resulted from the activity of the fault at the El Freno creek (Fig. 1). Finally the action of the humid weather in Neuquén Basin at those times (Melchor and Herbst, 2000; Hay et al., 1982; Wilson et al., 1994) could have led to the small scale fining- and thinning-upward units through increased sediment supply.

During the late Early Sinemurian the slope-type fan delta deposits at the top of El Pedrero section, the intermediate fan delta deposits at the top of Arroyo Malo section (Fig. 4) and the estuarine deposits at the base of Las Chilcas, De los Caballos and Codo del Blanco sections were deposited (Figs. 2 and 6 to 8). All these accumulations belong to the *Epophioceras* Zone (Riccardi et al., 2000) from late Early Sinemurian-Late Sinemurian age. The prograding mouth bars at the top of Arroyo Malo sec-

tion evidence a decrease of accommodation in late Early Sinemurian, but the mouth bars are contemporaneous with the estuarine deposits whose origin involves transgressions and increasing accommodation. This paradox can be explained considering the duration of 3 My of the *Epophiceras* Zone, long enough to allow a lowstand and a consequent sea level rise to occur. Besides, these sea level changes coincide with a lowstand and a sea level rise of the short term eustatic curve (Haq et al., 1987). The lowstand occurring at the end of the Early Sinemurian led to fluvial incision on the shelf and conglomerate deposition at the top of El Pedrero section (Fig. 14). A subsequent slow sea level rise caused an increase in accommodation on the hangingwall of the fault at the El Freno creek, allowing the mouth bars at the top of Arroyo Malo to prograde. Later a faster sea level rise and creation of accommodation allowed the flooding of the incised valleys and estuarine deposition in the Las Chilcas, De Los Caballos and Codo del Blanco sections.

Up to this point the late Early Sinemurian relative sea-level rise can be considered as a product of global eustasy. However the tectonic evolution of some neighbouring basement blocks of the Atuel-Valenciana half-graben (e.g. Dedos-Silla Block, Legarreta and Kozlowski, 1984) suggest the influence of subsidence. The Dedos-Silla Block is located 50 km towards the southwest from the study area at the present, and it has influenced the sedimentation up to cretaceous times (Legarreta and Kozlowski, 1984). Its first subsidence occurred by the late Early Sinemurian (Lanés, 2002), having no sedimentary record before that time. Another remarkable feature of the late Early Sinemurian relative sea-level rise is the spreading of the marine depositional area as the wave-dominated estuaries in most of the western sections confirm (Figs. 1 and 2). The spreading of the marine depositional area together with the subsidence of the Dedos-Silla Block at the late Early Sinemurian evidence the subsidence of a wider regional area and point to a regional sag. The late Early Sinemurian relative sea-level rise in the northern Neuquen basin was probably produced by a combination of an eustatic sea-level rise with a regional sag.

The late Early Sinemurian-Toarcian transgressive storm-dominated shelf evidences a steady creation of accommodation and an accommodation greater than the sediment supply. The equal amount of storm and fair-weather deposits at the eastern sections (Figs. 6 to 9) also confirms a broad accommodation because the storm waves of the offshore-shoreface transition zone cannot rework or erode the fair-weather deposits under these conditions. Then, an alternation of storm and fair-weather levels is formed. Retrograding pattern of the marine successions of late Early Sinemurian-Toarcian age is enhanced by the younging of their base toward the east due to a paleogeographic control (Fig. 2). At Codo del Blanco section the accommodation reached its maximum by the latest Pliensbachian (*Spinatum* Zone from the ammonite standard zones) when anoxic bottom waters and short dysaerobic events were recorded in laminated black shales with monoespecific pavements of *Bositra* sp. (Fig. 7). Pliensbachian anoxic bottom waters were likely due to the combination of a highstand and a "greenhouse effect" that led to a high nutrient flux toward the sea and an ocean circulation hindered by the latitudinal climatic homogeneity (Aberhan and Fürsich, 1997).

The aggradation vs. progradation and accommodation vs. sediment supply ratios allow identification of two stages of different tectonic behaviour: the first one during the Rhaetian-late Early Sinemurian and the second one during the late Early Sinemurian-Toarcian. The first stage showed an accommodation greater than the sediment supply and a rapid creation of accommodation responsible for the deposition of the slope-type fan deltas (Fig. 14). The late Early Sinemurian-Toarcian stage showed a variable accommodation; first the supply exceeded the accommodation allowing the progradation of intermediate fan delta mouth bars at late Early Sinemurian. Afterwards an accommodation greater than the supply, widespread marine depositional area and a slower creation of accommodation led to the development of the estuaries and transgressive marine shelf. The Rhaetian-late Early Sinemurian and late Early Sinemurian-Toarcian stages can be considered as synrift and sag phases respectively. The change from a fault-controlled subsidence to a thermal regime at the end of the Early Sinemurian explains the scarce accommodation needed to the progradation of the intermediate fan delta mouth bars.

The age of the synrift and sag phases proposed in this work are similar to the Norian-Middle Sinemurian age of the first rifting (Legarreta and Gulisano, 1989) and the Late Sinemurian-Late Pliensbachian age of the episode of thermal subsidence (Vergani et al., 1995). On the contrary, the synrift phase (Rhaetian-late Early Sinemurian) of this work also partially coincides with the postrift phase proposed by Spalletti (1997) and Spalletti et al. (1999) for a fluvio-lacustrine succession from the southern Atuel-Valenciana Half-graben. This fluvio-lacustrine succession records the evolution of a Norian anastomosed fluvial system to a Rhaetian anoxic lake. Spalletti (1997) attributed the anastomosed fluvial deposits to the synrift phase and the lacustrine ones to the post-rift (sag) phase.

CONCLUSIONS

Age and areal distribution allows the identification of two zones at the Atuel valley: one at the east of El Freno creek and the other to the west. Sections in the western area record the forestepping or shallowing event of sever-

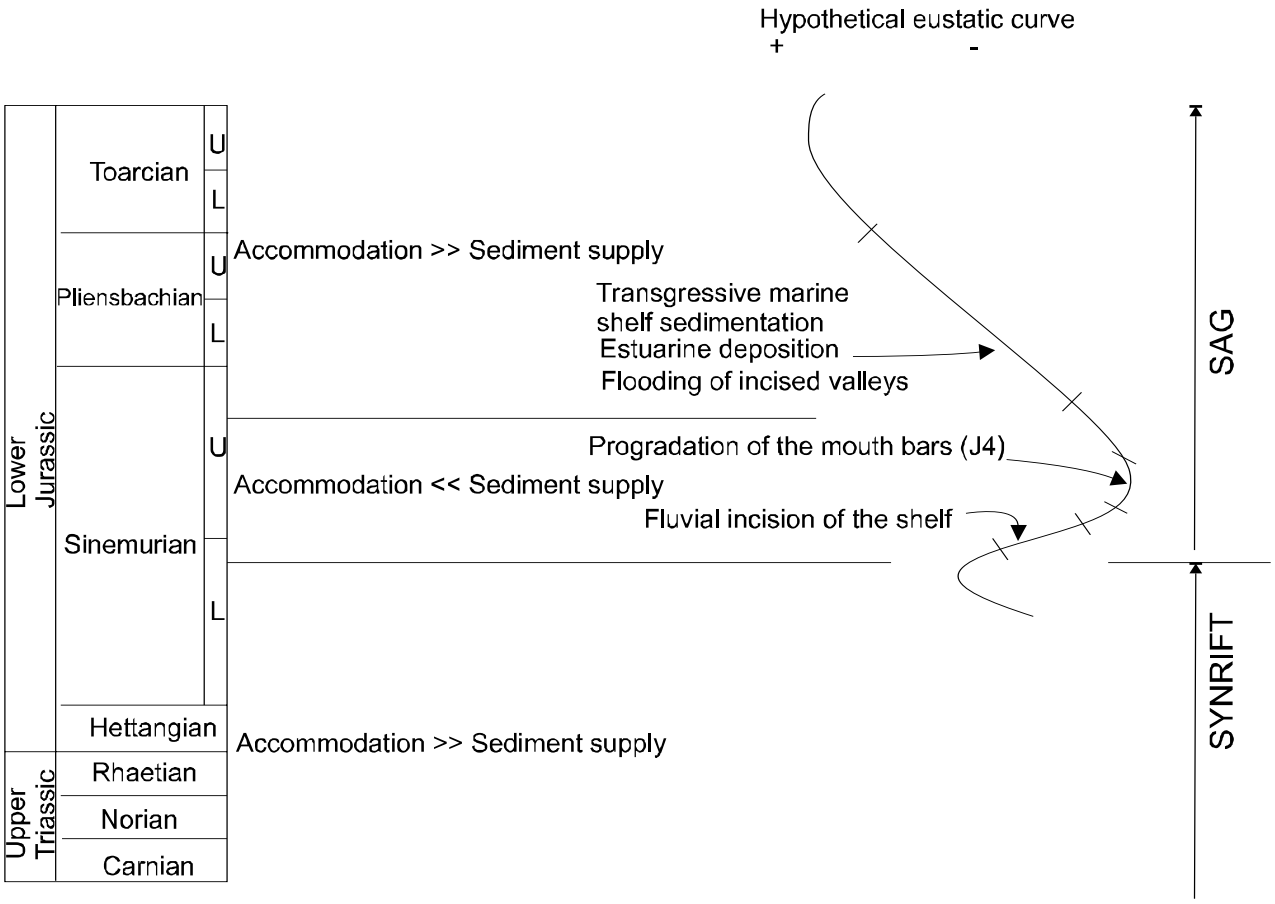

FIGURE 14 | **Late Triassic-Early Jurassic evolution of the accommodation vs. sediment supply proposed in this paper. A part of an hypothetical eustatic curve is given to show the eustasy-controlled changes of accommodation.**

al transverse, fault-controlled, fluvio-dominated slope-type fan deltas and, the progradation of an intermediate shelf to Gilbert-type fan delta, during the Rhaetian-late Early Sinemurian. Fan delta forestepping resulted from eustatic, tectonic and or climatic causes. Sections in the eastern area record a transgressive storm-dominated shelf, from wave-dominated estuaries to turbidity current influenced outer shelf, during the late Early Sinemurian-Toarcian.

Features and age of depositional systems, and inferred accommodation vs supply ratio and creation of accommodation rate, allow determination of two stages of different tectonic behaviour. The first stage (Rhaetian-late Early Sinemurian) had an accommodation greater than sedimentary supply, which led to the slope-type fan delta deposits. The second stage (late Early Sinemurian-Toarcian) showed a varying accommodation: during the late Early Sinemurian accommodation was outpaced by the sediment supply, allowing to the progradation of an intermediate fan delta and, later, during the late Early Sinemurian-Toarcian, accommodation exceeded the sediment supply again leading to the transgression of the marine shelf. The Rhaetian-late Early Sinemurian and late Early Sinemurian-Toarcian stages are considered as synrift and sag phases, respectively.

ACKNOWLEDGEMENTS

The author is deeply grateful to S. Damborenea, M. Manceñido, A. Riccardi (Universidad de La Plata y Museo) and A. Concheyro (Universidad de Buenos Aires) for the determinations of bivalves, brachiopods, ammonites, and calcareous nannofossil taxonomy, continuous orientation and support. To S. Hesselbo for valuable critics on the paper and written English, and (particularly) to D. Brown (associated editor) and A. Santos for continued assistance for the final version.

REFERENCES

Aberhan, M., Fürsich, F.T., 1997. Diversity analysis of Lower Jurassic bivalves of the Andean Basin and the Pliensbachian-Toarcian mass extinction. Letahia, 29, 181-195.

Ballance, P.F., 1988. The Huriwai braidplain delta of New

Zealand; a late Jurassic, coarse-grained, volcanic-fed depositional system in a Gondwana forearc basin. In: Nemec, W., Steel, R.J. (eds.). Fan deltas; Sedimentology and tectonic settings. Glasgow, Blackie and Sons, 430-444.

Behrendsen, O., 1921. Contribución a la geología de la pendiente oriental de la Cordillera Argentina. Actas de la Academia Nacional de Ciencias, 7, 161-227.

Bodenbender, G., 1892. Sobre el terreno Jurásico y Cretácico de los Andes Argentinos, entre el río Diamante y el río Limay. Boletín de la Academia Nacional de Ciencias, 13, 1-5.

Bornhold, B.D., Prior, D.B., 1990. Morphology and sedimentary processes on the subaqueous Noeick River delta, British Columbia, Canada. In: Colella, A., Prior, D.B. (eds.). Coarse-Grained Deltas. Oxford, International Association of Sedimentologists, Special Publication, 10, 169-181.

Brett, C.E., Baird, G.C., 1986. Comparative taphonomy; a key to paleoenvironmental interpretation on fossil preservation. Palaios, 1, 207-227.

Colella, A., 1988a. Pliocene–Holocene fan deltas and braid deltas in the Crati basin, southern Italy; a consequence of varying tectonic conditions. In: Nemec, W., Steel, R.J. (eds.). Fan deltas; Sedimentology and tectonic settings. Glasgow, Blackie and Sons, 50-74.

Colella, A., 1988b. Gilbert-type fan deltas in the Crati basin (Pliocene–Holocene, Southern Italy). In: Colella, A. (ed.). International Workshop on Fan Deltas, Calabria, Excursion Guidebook, Consiglio Nazionalle delle Ricerche, 19-77.

Changsog, L., Eriksson, K., Sitian, L., Youngxian, W., Jianye, R., Yanmey, Z., 2001. Sequence architecture, depositional systems, and controls on development of lacustrine basin fills in part of the Earlian Basin, northeast China. American Association of Petroleum Geologists Bulletin, 85, 2017-2048.

Chough, S.K., Hwang, I.G., 1997. The Duksung Fan Delta, SE Korea: growth of delta lobes on a Gilbert-type topsets, in response to relative sea-level rise. Journal of Sedimentary Research, 67, 725-739.

Dabrio, C.J., 1988. Fan-delta facies associations in Late Neogene and Quaternary basins of southeastern Spain. In: Nemec, W., Steel, R.J. (eds.). Fan deltas; Sedimentology and tectonic settings. Glasgow, Blackie and Sons, 91-111.

Dalrymple, R.W., Zaitlin, B.A., Boyd, R., 1992. Estuarine facies models; conceptual basis and stratigraphic implications. Journal of Sedimentary Petrology, 62, 1130-1146.

Dam, G., Surlyk, F., 1992. Forced regressions in a large wave- and storm-dominated anoxic lake, Rhaetian-Sinemurian Kap Stewart Formation, East Greenland. Geology, 20, 749-752.

Damborenea, S.E., 1987. Early Jurassic bivalvia of Argentina. Part 1: Stratigraphical introduction and Superfamilies Nuculanacea, Arcacea, Mytilacea and Pinnacea. Paleontographica, Abstracts, 199, 23-111.

Damborenea, S.E., 2002. Early Jurassic bivalves of Argentina, Part 3: Superfamilies Monotoidea, Pectinoidea, Plicatuloidea and Dimyoidea. Palaentographica, Abstracts, 265, 1-119.

Emery, D., Myers, K., 1996. Sequence Stratigraphy. Oxford, Blackwell Scientific Publications, 304 pp.

Ethridge, F.G., Wescott, W.A., 1984. Tectonic setting, recognition and hydrocarbon reservoir potential of fan-delta deposits. In: Koster, E.H., Steel, R.J. (eds.). Sedimentology of gravels and conglomerates. Calgary, Canadian Society of Petroleum Geologists, Memoir, 10, 217-235.

Field, M.E., Gardner, J.V., Prior, D.B., 1999. Geometry and significance of stacked gullies on the northern California Slope. Marine Geology, 154, 271-286.

Frostick, L.E., Steel, R.J., 1993. Tectonic signatures in sedimentary basin fills : an overview. In: Frostick, L.E., Steel, R.J. (eds.). Tectonic controls and signatures in sedimentary successions. Oxford, International Association of Sedimentologists, Special Publication, 20, 1-9.

Gawthorpe, R.L., Colella, A., 1988. Fan-delta facies associations in Late Neogene and Quaternary basins of southeastern Spain. In: Nemec, W., Steel, R.J. (eds.). Fan deltas; Sedimentology and tectonic settings. Glasgow, Blackie and Sons, 91-111.

Gawthorpe, R.L., Fraser, A.J., Collier, R.E.L., 1993. Sequence stratigraphy in active extensional basins: implications for the interpretation of ancient basin-fills. Marine and Petroleum Geology, 11, 642-658.

Gerth, E., 1925. Contribuciones a la estratigrafía y paleontología de los Andes Argentinos I. Estratigrafía y distribución de los sedimentos mesozoicos en los Andes Argentinos. Actas de la Academia Nacional de Ciencias, 9, 11-55.

Gloppen, T.G., Steel, R.J., 1981. The deposits, internal structure and geometry in six alluvial fan-fan delta bodies (Devonian-Norway)-a study in the significance of bedding sequence in conglomerates. In: Ethridge, F.G., Flores, R. (eds.). Recent and Ancient Nonmarine Depositional Environments: Models for Exploration. Tulsa, Society of Economic Paleontologists and Mineralogists, Special Publication, 31, 49-69.

Groeber, P., 1946. Observaciones Geológicas a lo largo del Meridiano 70º. 1- Hoja Chos Malal. Revista de la Asociación Geológica Argentina, 1, 177-208.

Groeber, P., 1947. Observaciones Geológicas a lo largo del Meridiano 70º. 2- Hojas Sosneao y Maipo. Revista de la Asociación Geológica Argentina, 2, 141-176.

Gulisano, C.A., 1981. El ciclo Cuyano en el norte de Neuquén y sur de Mendoza. San Luis, Actas del VIII Congreso Geológico Argentino, 3, 579-592.

Gulisano, C.A., Gutiérrez Pleimling, A.R., Digregorio, R.E., 1984. Esquema estratigráfico de la secuencia Jurásica del oeste de la provincia de Neuquén. San Carlos de Bariloche, Actas del IX Congreso Geológico Argentino, 1, 236-259.

Gulisano, C.A., Gutiérrez Pleimling, A.R., 1994. The Jurassic of the Neuquén Basin, b) Mendoza Province-Field Guide. Buenos Aires, Asociación Geológica Argentina, Serie E, 3, 103 pp.

Haq, B.U., Hardenbol, J., Vail, P.R., 1987. Chronology of fluctuating sea levels since the Triassic. Science, 235, 1156-1167.

Hay, W.W., Behensky, J.F. Jr, Barron, E.J., Sloan, J.L., 1982. LateTriassic - Liassic paleoclimatology of the Proto-central North Atlantic rift system. Palaegeography, Palaeoclimatology, Palaeoecology, 40, 13-30.

Holmes, A., 1965. Principles of Physical Geology. London, Thomas Nelson, 1288 pp.

Howell, J.A., Flint, S.S., 1996. A model for high resolution sequence stratigraphy within extensional basins. In: Howell, J.A., Aitken, J.F. (eds.). High resolution sequence stratigraphy: innovations and applications. London, Geological Society, Special Publication, 104, 129-137.

Jaworski, E., 1925. La fauna del Lías y Dogger de la Cordillera Argentina. Actas de la Academia Nacional de Ciencias, 9, 135-317.

Jervey, M.T., 1988. Quantitative geological modelling of siliciclastic rock sequences and their seismic expressions. In: Wilgus, C.K., Hastings, B.S., St. Kendall, C.G., Posamentier, H.W., Ross, C.A., Van Wagoner, J.C. (eds.). Sea level changes; an integrated approach. Tulsa, Society of Economic, Paleontologists and Mineralogists, Special Publication, 42, 235-254.

Kazanci, N., 1990. Fan-delta sequences in the Pleistocene and Holocene Burdur Basin, Turkey; the role of basin-margin configuration in sediment entrapment and differential facies development. In: Colella, A., Prior, D.B. (eds.). Coarse-Grained Deltas. Oxford, International Association of Sedimentologists, Special Publication, 10, 185-198.

Kleinspehn, K.L., Steel, R.J., Johannenssen, E., Netland, A., 1984. Conglomerate fan-delta sequences, Late Carboniferous-Early Permian, Western Spitsbergen. In: Koster, E.H., Steel, R.J. (eds.). Sedimentology of gravels and conglomerates. Calgary, Canadian Society of Petroleum Geologists, Memoir, 10, 279-294.

Kostaschuk, R.A., McCann, S.B., 1987. Subaqueous morphology and slope processes in a fjord delta, Bella Coola, British Columbia. Canadian Journal of Earth Sciences, 24, 52-59.

Lanés, S., 2002. Paleoambientes y paleogeografía de la primera transgresión en Cuenca Neuquina. Doctoral thesis. Universidad de Buenos Aires, 403 pp.

Legarreta, L., Gulisano, C. A., 1989. Análisis estratigráfico de la cuenca Neuquina (Triásico superior-Terciario inferior). In: Chebli, G.A., Spalletti, L.A. (eds.). Cuencas Sedimentarias Argentinas. San Miguel de Tucumán, Instituto Miguel Lillo, Universidad Nacional de Tucumán, Serie de Correlación Geológica, 6, 221-244.

Legarreta, L., Gulisano, C.A., Uliana, M.A., 1993. Las secuencias sedimentarias Jurásico-Cretácicas. In: Ramos, V.A. (ed.). Geología y Recursos naturales de Mendoza. Mendoza, XII Congreso Geológico Argentino y II Congreso de Exploración de Hidrocarburos, 87-114.

Leithold, E.L., Bourgeois, J., 1984. Characteristics of coarse-grained sequences deposited in nearshore, wave dominated environments-Examples from the Miocene of southwestern Oregon. Sedimentology, 31, 749-775.

Lowe, D.R., 1982. Sediment gravity flows: Depositional models with special reference to the deposits of high-density turbidity currents. Journal of Sedimentary Petrology, 52, 279-297.

Manceda, R., Figueroa, D., 1993. La inversión del rift mesozoico en la Faja Fallada y Plegada de Malargüe, provincia de Mendoza. Mendoza, Actas del XII Congreso Geológico Argentino y II Congreso de Exploración de Hidrocarburos, 3, 219-232.

Manceda, R., Figueroa, D., 1995. Inversion of the Mesozoic Neuquén Rift in the Malargüe Fold and Thrust Belt, Mendoza. Argentina. In: Tankard, A.J., Suárez Soruco, R., Welsink, H.J. (eds.). Petroleum Basins of South America. Tulsa, American Association of Petroleum Geologists, Memoir, 62, 369-382.

Massari, F., Colella, A., 1988. Evolution and types of fan-delta systems in some major tectonic settings. In: Nemec, W., Steel, R.J. (eds.). Fan deltas; Sedimentology and tectonic settings. Glasgow, Blackie and Sons, 103-122.

Mastalerz, K., 1995. Deposits of high-density turbidity currents on fan-delta slopes: an example from the Upper Visean Szczawno Formation, Intrasudetic Basin, Poland. Sedimentary Geology, 98, 121-146.

Mc Callum, J.E., Robertson, A.H.F., 1995. Sedimentology of two fan-delta systems in the Pliocene-Pleistocene of the Mesaoria Basin, Cyprus. Sedimentary Geology, 98, 215-244.

Melchor, R.N., Herbst, R., 2000. Sedimentology of the El Puquén Formation (Upper Triassic, central Chile) and the new plant *Mollesia melendezia* gen. et sp. nov. (Pteridophylla, incertae sedis). Ameghiniana, 37, 477-485.

Mulder, T., Syvitski, J.P.M., 1995. Turbidity currents generated at river mouths during exceptional discharges to the world oceans. Journal of Geology, 103, 285-299.

Mulder, T., Syvitski, J.P.M., Skene, K.I, 1998. Modeling of erosion and deposition by turbidity currents generated at river mouths. Journal of Sedimentary Research, 68, 124-137.

Muto, T., 1993. Incised valleys in the Pleistocene Tenryugawa and Oigawa coastal-fan systems, central Japan. The concept of the fan valley interval. In: Posamentier, H.W., Summerhayes, C.P., Haq, B.U., Allen, G.P. (eds.). Sequence stratigraphy and facies associations. Oxford, International Association of Sedimentologists, Special Publication, 18, 69-92.

Mutti, E., 1992. Turbidite Sandstones. Milan, AGIP - Istituto di Geologia Universitá di Parma, 275 pp.

Mutti, E., Davoli, G., Tinterri, R., Zavala, C., 1996. The importance of ancient fluvio-deltaic systems dominated by catastrophic flooding in tectonically active basins. Memoria Sciencia Geologica, 48, 233-291.

Mutti, E., Tinterri, R., Remacha, E., Mavilla, N., Angella, S., Fava, L., 1999. An introduction to the analysis of ancient turbidite basins from an outcrop perspective. Tulsa, American Association of Petroleum Geologists, Continuing Education Course Note Series, 39, 61 pp.

Nemec, W., Steel, R.J., 1988. What is a fan delta and how do we recognize it? In: Nemec, W., Steel, R.J. (eds.). Fan deltas; Sedimentology and tectonic settings. Glasgow, Blackie and Sons, 3-13.

Normark, W.R., Piper, D.J.W., 1991. Initiation processes and flow evolution of turbidity currents: implications for the depositional record. In: Osborne, R.H. (ed.). From Shoreline to Abyss. Tulsa, Society of Economists Paleontologists Mineralogists, Special Publication, 46, 207–227.

Orton, G.J., 1988. A spectrum of Middle Ordovician fan deltas and braidplain deltas, North Wales; a consequence of varying fluvial clastic input. In: Nemec, W., Steel, R.J. (eds.).

Fan deltas; Sedimentology and tectonic settings. Glasgow, Blackie and Sons, 23-49.

Posamentier, H.W., Allen, G.P., 1993a. Variability of the sequence stratigaphic model; effects of local basin factors. Sedimentary Geology, 86, 91-109.

Posamentier, H.W., Allen, G.P., 1993b. Siliciclastic sequence stratigraphic patterns in foreland ramp type basins. Geology, 21, 455-458.

Postma, G., 1990a. Depositional architecture and facies of river and fan deltas : a synthesis. In: Colella, A., Prior, D.B. (eds.). Coarse-Grained Deltas. Oxford, International Association of Sedimentologists, Special Publication, 10, 13-27.

Postma, G., 1990b. An analysis of the variation in delta architecture. Terra Nova, 2, 124-130.

Prior, D.B., Bornhold, B.D., Wiseman, W.J., Lowe, D.R., 1987. Turbidity current activity in a British Columbia Fjord. Science, 237, 1330-1333.

Prior, D.B., Bornhold, B.D., 1989. Submarine sedimentation on a developing Holocene fan delta. Sedimentology, 36, 1053-1076.

Prior, D.B., Bornhold, B.D., 1990. The underwater development of Holocene fan deltas. In: Colella, A., Prior, D.B. (eds.). Coarse-Grained Deltas. Oxford, International Association of Sedimentologists, Special Publication, 10, 75-90.

Prior, D.B., Wiseman, W.J., Bryant, W.R., 1981. Submarine chutes on the slopes of fjord deltas. Nature, 290, 326-328.

Ramos, V.A., 1992. Geología de la Alta Cordillera de San Juan. Revista de la Asociación Geológica Argentina, 47, 268-269.

Rasmussen, E., 1997. Depositional evolution and sequence stratigraphy of the shelf and slope area off south Gabon, West Africa. Journal of Sedimentary Research, 67, 715-724.

Ravnås, R., Steel, R.J., 1998. Architecture of marine rift-basins successions. American Association of Petroleum Geologists Bulletin, 82, 110-146.

Reading, H.G., Collinson, J.D., 1996. Clastic coasts. In: Reading, H.G. (ed.). Sedimentary environments; Processes, Facies and Stratigraphy. Oxford, Blackwell Scientific Publications, 154-231.

Reijenstein, C., 1967. Estratigrafía y tectónica de la zona al norte del río Atuel entre los arroyos Blanco y Malo (Provincia de Mendoza). Trabajo Final de Licenciatura. Universidad de Buenos Aires, 97 pp.

Reinson, G.E. 1992. Transgressive barrier island and estuarine systems. In: Walker, R.G., James, N.P. (eds.). Facies Models, Response to sea level change. St. Johns, Geological Association of Canada, 179-194.

Riccardi, A., Damborenea, S., Manceñido, M.O., Ballent, S.C., 1988. Hettangiano y Sinemuriano marinos en Argentina. Santiago, Actas del V Congreso Geológico Chileno, 2, 359-377.

Riccardi, A., Damborenea, S., Manceñido, M.O., Ballent, S.C., 1991. Hettangian and Sinemurian (Lower Jurassic) biostratigraphy of Argentina. Journal of South American Earth Sciences, 4, 159-170.

Riccardi, A., Damborenea, S.E., Manceñido, M.O., Scasso, R., Lanés, S., Iglesia Llanos, P., Stipanicic, P.N., 1997. Primer registro de Triásico marino fosilífero de la Argentina. Revista de la Asociación Geológica Argentina, 52, 228-234.

Riccardi, A.C., Iglesia Llanos, M.P., 1999. Primer hallazgo de amonites en el Triásico de la Argentina. Revista de la Asociación Geológica Argentina, 54, 298-300.

Riccardi, A.C., Leanza, H.A., Damborenea, S., Manceñido, M.O., Ballent, S.C., Zeiss, A., 2000. Marine Mesozoic Biostratigraphy of the Neuquén Basin. In: Miller, H., Hervé, F. (eds.). Zeitschrift für Angewandte Geologie SH1. Rio de Janeiro, 31st. International Geological Congress, 103-108.

Rosenfeld, V., Volkheimer, W., 1981. Jurassic turbidites in central western Argentina (Neuquén Basin). In: Cresswell, M.M., Vella, P. (eds.). Gondwana Five. Rotterdam, Balkema, 155-160.

Soh, W., Tanaka, T., Taira, S., 1995. Geomorphology and sedimentary processes of a modern slope-type fan delta (Fujikawa fan delta), Suruga Trough, Japan. Sedimentary Geology, 98, 79-95.

Spalletti, L.A., 1997. Sistemas deposicionales fluvio-lacustres en el rift Triásico de Malargüe (sur de Mendoza, República Argentina). Anales de la Academia Nacional de Ciencias Exactas, Físicas y Naturales, 49, 109-124.

Spalletti, L.A., Artabe, A., Morel, E., Brea, M., 1999. Biozonación paleoflorística y cronoestratigrafía del Triásico argentino. Ameghiniana, 36, 419-451.

Steckler, M.S., Reynolds, D.J., Coakley, B.J., Swift, B.A., Jarrards, R.,1993. Modelling passive margin sequence stratigraphy. In: Posamentier, H.W., Summerhayes, C.P., Haq, B.U., Allen, G.P. (eds.). Sequence stratigraphy and facies associations. Oxford, International Association of Sedimentologists, Special Publication, 18, 19-41.

Steel, R.J., 1988. Coarsening-upward and skewed fan bodies: symptoms of strike-slip and transfer fault movement in sedimentary basins. In: Nemec, W., Steel, R.J. (eds.). Fan deltas; Sedimentology and tectonic settings. Glasgow, Blackie and Sons, 75-83.

Steuer, A., 1921. Estratos Jurásicos argentinos. Contribución al conocimiento de la Geología y Paleontología de los Andes argentinos entre el río Grande y el río Atuel. Actas de la Academia Nacional de Ciencias, 7, 25-129.

Stipanicic, P.N., 1969. El avance en los conocimientos del Jurásico argentino a partir del esquema de Groeber. Revista de la Asociación Geológica Argentina, 24, 367-388.

Stipanicic, P.N., Bonetti, M.I.R., 1970. Posiciones estratigráficas y edades de las principales floras jurásicas argentinas. Ameghiniana, 7, 57-78.

Surlyk, F., 1984. Fan-delta to submarine fan conglomerates of the Volgian-Valanginian Wollastone Forland Group, East Greenland. In: Koster, E.H., Steel, R.J. (eds.). Sedimentology of gravels and conglomerates. Calgary, Canadian Society of Petroleum Geologists, Memoir, 10, 359-362.

Tankard, A.J., Uliana, M.A., Welsink, H.J., Ramos, V.A., Turic, M., França, A.B., Milani, E.J., Brito Neves, B.B., Eyles, N., Skarmeta, J., Santa Ana, H., Wiens, F., Cirbián, M., López Paulsen, O., Germs, G.J.B., De Wit, M.J., Machacha, T., Miller, R., 1995. Structural and tectonic controls of basin

evolution in southwestern Gondwana during the Phanerozoic. In: Tankard, A.J., Suárez Soruco, R., Welsink, H.J. (eds.). Petroleum Basins of South America. Tulsa, American Association of Petroleum Geologists, Memoir, 62, 5-52.

Uliana, M.A., Biddle, K.T., 1988. Mesozoic-Cenozoic paleogeographical and geodynamic evolution of southern South America. Revista Brasileira de Geociências, 18, 172-190.

Vergani, G.D., Tankard, A.J., Belotti, H.J., Welsink, H.J., 1995. Tectonic evolution and paleogeography of the Neuquén Basin, Argentina. In: Tankard, A.J., Suárez Soruco, R., Welsink, H.J. (eds.). Petroleum Basins of South America. Tulsa, American Association of Petroleum Geologists, Memoir, 62, 383-402.

Volkheimer, W., 1978. Descripción Geológica de la Hoja 27 a, Cerro Sosneado, provincia de Mendoza. Boletín No. 151, Buenos Aires, Servicio Geológico Nacional, 83 pp., 1 fold map.

Wehrli, L., Burckhardt, C., 1898. Rapport préliminaire sur une expédition géologique dans la Cordilliere Argentino-Chilienne, entre le 33° et 36° latitude sud. Revista del Museo de La Plata, 8, 373-388.

Weinrich, F.H., 1989. The generation of turbidity currents by subaerial debris flows, California. Geological Society of America Bulletin, 101, 278-291

Wheatcroft, R.A., Sommerfeld, C.K., Drake, D.E., Borgeld, J.C., Nittrouer, C.A., 1997. Rapid and widespread dispersal of flood sediment on the northern California margin. Geology, 25, 163-166.

Wilson, K.M., Pollard, D., Hay, W.W., Thompson, S.L., Wold, C.N., 1994. General circulation model simulations of Triassic climates: Preliminary results. In: Klein, G. (ed.). Pangea: Paleoclimate, Tectonics and Sedimentation during accretion, zenith and breakup of a supercontinent. Boulder, Geological Society of America, Special Paper, 288, 91-116.

Manuscript received August 2003;
revision accepted September 2004.

APPENDIX

Description and interpretacion of facies associations

TABLE 1 | **Facies associations of the Rhaetian-Middle Hettangian cycle at Arroyo Malo section.**

Name	Deposits	Depositional processes paleoenvironment
T1	Plane laminated mudstones, Tde and Tce turbidites (Figs. 10a, 10b). Mudstone concretions	Mud deposition and low-density turbidity currents. Basin area far from fan delta front
T2	Tce, Tbe and Tde turbidites, plane laminated mudstones. Mudstone concretions.	Low-density turbidity currents and mud deposition. Slope-type fan delta prodelta
T3	Tae, Tac, Tbe, Tce and Tde turbidites, laminated mudstones, massive pebbly mudstones, intraformational breccias (Fig. 10d), massive clast- and mud-supported conglomerates. Tae and Tac turbidites with dense lithics. Lenses of trough-cross bedded sandstones. Sediment deformation (slumps, slump folds, faults, convolute lamination, fluid escape structures, pseudonodules, load deformation and syneresis cracks) (Fig. 10c).	Low-density and high-density turbidity currents, mud deposition, cohesive debris flows (some of them derived from slumps or resedimented fluvial deposits). Channelized low-regime traction flows. Lower part of a steeply (Slope-type) fan delta front.
T4	Usually amalgamated tabular deposits and lenses (10-20 m wide, 0,4-1 m thick) filled with massive pebbly mudstones, Tbe, Tde, Tce and Tae turbidites and plane laminated mudstones. Lenses cut stackings of Tbe, Tde and Tce turbidites.	Cohesive debris flows, low-density and high-density turbidity currents and mud deposition. Chutes and inactive interchute areas in the slope-type fan delta front, below wave base.
T5	Lenses (10-100 m wide, 0,5-3 m thick) filled with trough-cross bedded sandstones, shell lenses, normal graded clast-supported conglomerates, massive pebbly sandstones, Ta turbidites with mudclasts or shells, Tac and Tae turbidites with dense lithics, at the bases; and Tce, Tde, Tbe turbidites and plane laminated mudstones at the lense tops. Lenses alternate with tabular beds of intraformational breccia and massive mud-supported conglomerates.	Hyperconcentrated flows, high-density and low-density turbidity currents and channelized low-regime traction flows. Unconfined cohesive debris flows derived from the slumping of turbidite or fluvial successions. Braided distributary channels, inactive interdistributary areas, and levees in the slope-type fan delta upper front, below wave base.

TABLE 2 | **Facies associations of Middle Hettangian-middle Late Hettangian and middle Late Hettangian-late Early Sinemurian cycles at Arroyo Malo and El Pedrero sections.**

Name	Deposits	Depositional processes paleoenvironment
J1	Tbe, Tce, Tde turbidites, plane laminated mudstones and less Tae turbidites. Mudstone concretions. (Fig. 11a).	Mud deposition, low-density and high-density turbidity currents. Slope-type fan delta prodelta.
J2	Tabular beds and lenses filled with Tae, Ta, Tbe, Tce and Tde turbidites, massive sandstones, intraformational breccias and sandstones with isolated tangential 2-D dunes (Fig. 11c). Sediment deformation (slump folds, convolute lamination, faults, fluid escape structures, sedimentary boudinage pseudonodules, load deformation and syneresis cracks). (Figs. 11d, 11e, 11f)	Low-density and high-density turbidity currents, high-density turbidity currents which suffered an hydraulic jump and small amount of cohesive debris flows derived from slumps. Inactive interchute areas and some chutes in the slope-type fan delta lower front.
J3	Usually amalgamated Tae, Tac and Ta turbidites, massive pebbly mudstones and less Tbe, Tce and Tde turbidites.	High-density and low-density turbidity currents, cohesive debris flows. Slope-type fan delta lower front.
J4	Tabular beds of tangential cross-bedded sandstones (Fig. 11g) cut by lenses filled with trough-cross bedded, plane laminated and parting lineated sandstones. Tabular Tce, Tde and Tbe turbidites.	Unconfined and channelized low-regime traction flows, low-density turbidity currents. Mouth bars and distributary channels of an intermediate (shelf to Gilbert-type) fan delta front.
J5	Tabular beds or usually amalgamated lenses filled with Ta (Fig. 11b) and Tae turbidites. Multiepisodic or simple lenses (10-100 m wide, 1-3 m thick) filled with normal graded and plane laminated clast-supported conglomerates (sometimes with mud clasts and inversely-graded laminae) or trough-cross bedded sandstones. Stacked Tce, Tbe and Tde turbidites, and some sandstones with isolated tangential 2-D dunes (Fig. 11c).	High-density and low-density turbidity currents, high-density turbidity currents that suffered a hydraulic jump, channelized hyperconcentrated flows and some channelized low-regime traction flows. Chutes, some distributary channels, inactive interdistributary areas of a slope-type fan delta front.
J6	Multiepisodic or simple lenses (10-100 m wide, 0,5-3 m thick) filled with normal graded clast-supported conglomerates, trough-cross bedded conglomerates or trough-cross bedded sandstones with shell lenses, underlaying Tbe and Tce turbidites. Interfingering with stacked Tbe and Tce turbidites.	Channelized low-regime and upper-regime traction flows and channelized hyperconcentrated flows. Braided distributary channels, levees and inactive interdistributary areas of a slope-type fan delta front, below wave base.

TABLE 3 | **Facies associations of late Early Sinemurian-Toarcian age at eastern sections. J10 and J11 only appear at the tops of Las Chilcas and Codo del Blanco sections.**

Name	Deposits	Depositional processes paleoenvironment
J7	Lenses filled with herringbone cross-bedded sandstones and shell lags (Fig. 12d), basal massive or normal graded clast-supported conglomerates and trough-cross bedded sandstones at the top (Figs. 12a, 12b). Some lenses are multiepisodic. Tabular beds of tangential cross-bedded sandstones with mud drapes (Figs. 11e, 11f); trough cross-bedded sandstones, swash cross-bedded sandstones with plane lamination and parting lineation. De los Caballos section: also trough cross-bedded sandstones with wave ripples and shell lags, swaley cross-stratified sandstones. Codo del Blanco section: tabular amalgamated hummocky cross-stratified sandstones, swash cross-bedded sandstones, trough cross-bedded sandstones with wave ripples and shell lags, plane laminated and parting lineated sandstones, planar cross-bedded sandstones. Lenses filled with bipolar imbricated conglomerates (Fig. 12c) and freshwater bivalves (*Cardinioides* n. sp., Damborenea, pers. comm.); tabular beds of massive or normally graded shelly sandstones, less massive fine sandstones, massive mudstones and plane laminated shales.	Tidal inlets and tidal sand waves in the subtidal to lower intertidal area of a wave-dominated estuary. De los Caballos creek : also small amount of fairweather and storm wave deposits above fairweather wave base. Wave-dominated estuary. Conglomeratic tidal inlets, fairweather and storm wave and current deposits above fairweather wave base. External wave dominated estuary Small amount of mudstone and washover fans of the central wave-dominated estuary.
J8	Tabular amalgamated beds of massive or normally graded shelly sandstones, hummocky cross-stratified sandstones (Fig. 13b) and swaley cross-stratified sandstones (Fig. 13a). Tabular beds of trough cross-bedded sandstones with wave ripples (Fig. 13c), swash cross-bedded sandstones and less massive fine sandstones.	Fairweather and storm waves and currents, low energy fairweather currents around the fairweather wave base. Shoreface to upper offshore-shoreface transition zone of a storm-dominated shelf.
J9	Tabular single beds of hummocky cross-stratified sandstones (Fig. 13f); massive fine sandstones with pavements of epifaunal bivalves, brachiopods and serpulids in life position; normally graded and plane laminated coarse sandstones. Small amount of massive sandstones with clumps of brachiopods in life position and massive mudstones.	Storm waves and currents, low energy fairweather currents and mudstone deposition around the storm-wave base. Offshore-shoreface transition zone and upper offshore of a storm-dominated shelf.
J10*	Massive mudstones and laminated shales, normally graded and plane laminated medium sandstones. Small amount of Tce, Tde, Tbe, Tae and Tac turbidites.	Mudstone deposition and small amount of low-density and high-density turbidity currents below storm wave base. Turbidity current-influenced offshore on the inner-shelf.
J11*	Tce, Tbe and Tde turbidites, massive mudstones and laminated shales. Small amount of Tae and Tac turbidites, tabular massive sandy mudstones and wide lenses filled with normally graded clast-supported conglomerates and trough cross-bedded sandstones.	Mudstone deposition, high-density and low-density turbidity currents, sandy debris flows, hyperconcentrated flows with tops reworked by low-regime traction currents. Turbidity current-influenced outer shelf.